Biochemical Characterization of the two-component monooxygenase system: Isobutylamine *N*-hydroxylase (IBAH) and Flavin reductase (FRED)

Benedicta Forson

Thesis submitted to the faculty of Virginia Polytechnic Institute and State University in partial fulfillment of the requirements for the degree of

Master of Science

In

Life Science in Biochemistry

Pablo Sobrado, Chair
Robert H White
Bin Xu
Daniel Slade

April 29, 2016
Blacksburg, VA

Keywords: Isobutylamine *N*-hydroxylase (IBAH), flavin reductase (FRED), oxidation, hydroxylation, *Streptomyces viridifaciens*, valanimycin

Biochemical Characterization of the two-component monooxygenase system: Isobutylamine *N*-hydroxylase (IBAH) and Flavin reductase (FRED)

Benedicta Forson

ABSTRACT

Isobutylamine *N*-hydroxylase (IBAH) and flavin reductase (FRED) from *Streptomyces viridifaciens* are part of a two-component flavin-dependent monooxygenase enzyme system that catalyze the conversion of isobutylamine (IBA) to isobutylhydroxylamine (IBHA), a key step in the formation of valanimycin, an azoxy antibiotic. In this work, we present the over-expression, purification and biochemical characterization of this two-component enzyme system. IBAH and FRED were expressed and purified to homogeneity as separate proteins. FRED exhibited the oxidoreductase activity by catalyzing the oxidation of NADPH. The hydroxylation activity of IBAH was confirmed using liquid chromatography – mass spectrometry (LC-MS). Steady state kinetic data showed an oxidation activity of the monooxygenase component which proceeded at 1.97 ± 0.06 s^{-1} as measured from oxygen consumption and in product formation, the rate was 0.012 ± 0.001 s^{-1}, suggesting a high degree of uncoupling between product formation and oxygen consumption. In pre-steady state kinetic characterization studies, the FRED-catalyzed reduction of FAD by NADPH occurred at a rate of 10.0 ± 0.2 s^{-1} and the K_M was 490 ± 40 μM. The rate of reduction was ~1.5-fold decreased in the presence of substrate IBA whiles the K_M was 500 ± 50 μM. NADH showed a markedly reduced rate of reduction with a k_{red} of 0.34 ± 0.03 s^{-1} with an apparent K_M of 3000 ± 500 μM. The rate of flavin re-oxidation in the absence of monooxygenase IBAH was 4.79×10^{-9} $M^{-1}s^{-1}$. Our results suggest a reaction mechanism for the IBAH monooxygenase system controlled by the oxidation half reaction that may be modulated by a complex formation between the reductase and monooxygenase components.

ACKNOWLEDGEMENTS

I would like to thank the Almighty God for his grace to be able to complete this degree. I would also like to thank my advisor Dr. Pablo Sobrado, for the opportunity to work in his laboratory and for his tireless efforts, guidance and patience during my graduate education. Also to my committee members; Dr. Robert White, Dr. Bin Xu and Dr. Daniel Slade whose immense guidance has aided in the successful completion of this work. To the members of the Sobrado lab, Dr. Isabel Da Fonseca, Dr. Julia Del Martin-Campo, Heba Annis, Mynor Medrano and Maddie Marcus. Your contribution in diverse ways towards this thesis cannot go unrecognized. Thank you! To Kim Harich, who was very instrumental in the analysis and understanding of mass spectrometry data. Finally to my family the Forsons and friends for their support in diverse ways to the completion of my Masters thesis.

TABLE OF CONTENTS

CHAPTER 1: Introduction

1.1 Flavin dependent monooxygenases

Flavin dependent monooxygenases are involved in catalysis of a wide range of biological reactions including catabolism of natural and anthropogenic compounds, biosynthesis of antibiotics and hormones, and some have been found useful as druggable targets due to the essential nature of the reactions they catalyze [1, 2]. Flavin dependent monooxygenases catalyze the incorporation of one atom of molecular oxygen into their substrates, while the other oxygen atom is reduced to water. The mechanism of activation of the oxygen molecule typically involves the formation of a transiently stable C4a-(hydro)peroxyflavin; a covalent adduct which upon protonation or deprotonation, serves as an electrophile or neutrophile for oxygenation of the target substrate. Figure 1 shows a scheme for activation of oxygen in flavin dependent monooxygenases [3]. The C4a-(hydro)peroxyflavin intermediate formed is usually unstable and decays to form hydrogen peroxide and oxidized flavin. However, flavin monooxygenases have developed mechanisms by which they stabilize this adduct in order to be able to oxygenate their substrates [4]. These enzymes catalyze among others; hydroxylation, Baeyer-Villiger oxidation, sulfoxidation, epoxidation, and halogenation reactions [5].

The first monooxygenase to be characterized was lactate dehydrogenase (EC 1.13.12.4) in 1957 and since its successful expression, purification and characterization, [6] at least 130 flavin-dependent monooxygenases have been characterized. Due to their high selectivity they have been found useful in industrial applications as potential enantioselective biocatalysts for the synthesis of high value chemicals [1]. A thorough elucidation of the structural bases that govern the functional properties of

monooxygenases is crucial in addressing one of the most fascinating issues in flavoenzymology, the ability of flavoenzymes to activate or react with molecular oxygen [7].

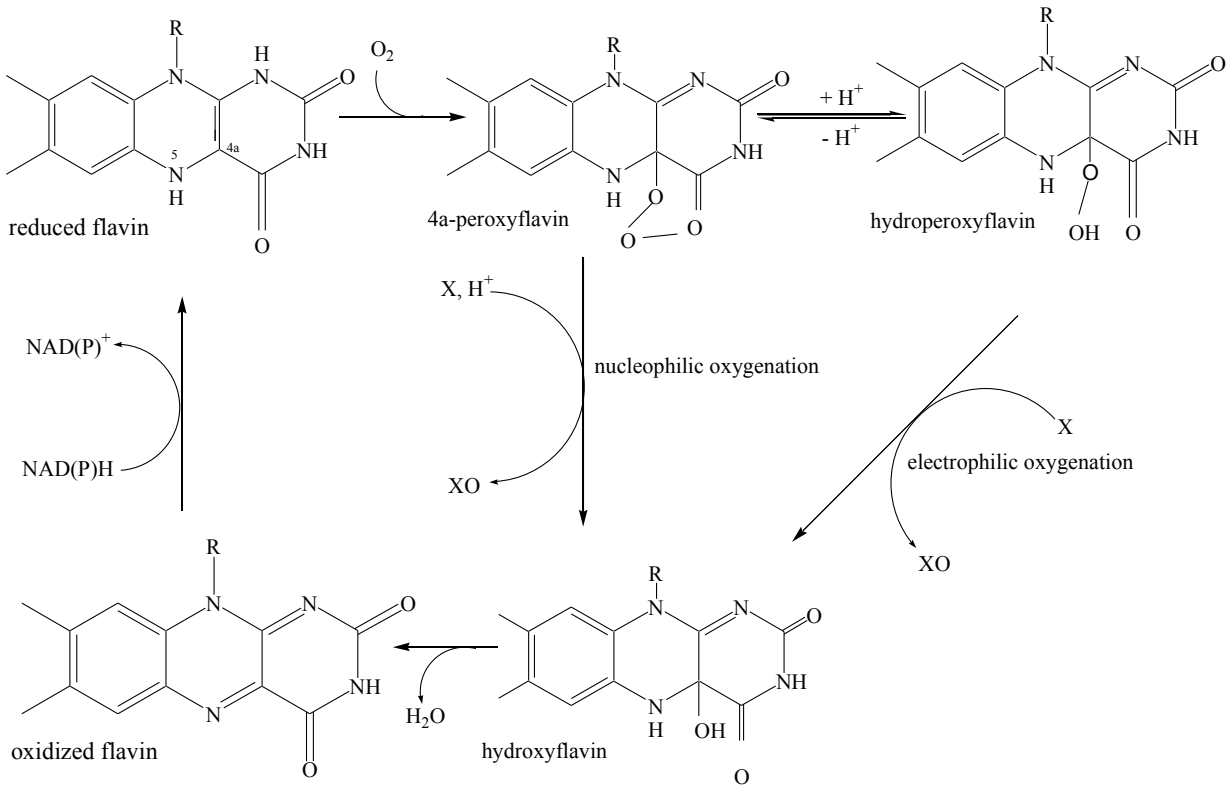

Figure 1. Mechanism of oxygen activation in flavin-dependent monooxygenases.

1.2 Classification of flavin dependent monooxygenases

Classification of flavoenzymes is based on criteria such as: the type of chemical reaction that is catalyzed, the nature of the reducing and oxidizing substrates, structural features, electron donor and type of oxygenation reaction [8, 9]. Based on these criteria, eight groups (A, B, C, D, E, F, G and H) have been described. A summary of their cofactors, electron donors, protein fold and the reactions they catalyze, as well as some common prototypes are listed in table 1 [1]. Group A flavin-dependent monooxygenases are encoded by a single gene and contain a tightly bound FAD cofactor. Group B monooxygenases can

be divided into Baeyer-Villiger monooxygenases (BVMOs), *N*-hydroxylating monooxygenases (NMOs) and flavin-containing monooxygenases (FMOs) [10, 11]. Groups C – F are encoded by multiple genes encoding one or two monooxygenase components and a reductase component. The reduced flavin is supplied by the reductase component for the enzymes in these groups [9]. In group G monooxygenases, the enzymes rely on an amino acid substrate as the electron donor for the reaction. The reaction involves cleavage of an α-CH bond of the amino acid, followed by a transfer of a hydride equivalent to FAD to form the enzyme-bound imino acid [12]. The last group of monooxygenases is the Group H members, who like Group F monooxygenases, also reduce the flavin cofactor through substrate oxidation.

TABLE 1

Classification of flavin dependent monooxygenases

Group	Cofactor	Electron donor	Protein fold	Reaction	Prototype
A	FAD	NAD(P)H	Rossmann (GR-2)	Hydroxylation Sulfoxidation	*p*-Hydroxybenzoate 3-hydroxylase MICAL[a]
B	FAD	NAD(P)H	Rossmann (FMO)	Baeyer–Villiger oxidation Heteroatom oxygenation N-Hydroxylation Oxidative decarboxylation	Cyclohexanone monooxygenase Dimethylaniline monooxygenase L-Ornithine monooxygenase Indole-3-pyruvate monooxygenase
C	FMN	$FMNH_2$	TIM barrel	Light emission Baeyer–Villiger oxidation Epoxidation Desulfurization Sulfoxidation Hydroxylation	Diketocamphane monooxygenase Alkanesulfonate monooxygenase Long-chain alkane monooxygenase
D	FAD/FMN	$FADH_2$/$FMNH_2$	Acyl coA dehydrogenase	Hydroxylation N-Hydroxylation	*p*-Hydroxyphenylacetate 3-hydroxylase KijD3 sugar oxygenase
E	FAD	$FADH_2$	Rossmann (GR-2)	Epoxidation	Styrene monooxygenase
F	FAD	$FADH_2$	Rossmann (GR-2) [b]	Halogenation	Tryptophan 7-halogenase
G	FAD	Substrate	Rossmann (MAO) [c]	Oxidative decarboxylation	Tryptophan 2-monooxygenase
H	FMN	Substrate	TIM barrel (glycolate oxidase)	Oxidative decarboxylation Oxidative denitration	Lactate 2-monooxygenase Nitronate monooxygenase

[a]MICAL - Molecule interacting with CasL

[b]MAO – monoamine oxidase

[c]GR- glutathione reductase

1.3 Structural and mechanistic characteristics of the best known classes of monooxygenases

Among the eight classes of flavin dependent monooxygenases that are known, few enzymes have been extensively characterized in each group. However, members of Groups A, B, C and F have been extensively studied and their catalytic mechanisms and structures have been elucidated.

Group A monooxygenases catalyze regioselective ortho or para hydroxylation of phenolic compounds. They require NADPH as their electron donor and the $NADP^+$ is released immediately upon flavin reduction [9]. *p*-hydroxybenzoate hydroxylase is a well-characterized member in this group. Mechanistic and structural insight into this enzyme revealed the absence of a recognizable domain for NADPH binding. Crystallographic analysis of the structure established the enzyme as a monomer with three discernible domains. A high-resolution structure of the active site of the oxidized enzyme complexed with its aromatic substrate shows multiple contacts between enzyme and substrate. The substrate lies in below the N-5 position of the flavin ring. The arrangement of residues in the active site permits the peroxide intermediate of flavin to rotate into a position to allow reaction with the substrate. These results buttressed observations from the oxidative reaction in the catalytic cycle [4].

Group B flavin monooxygenases, have an α/β Rossmann fold which respectively bind FAD and NAD(P)H. In contrast to Group A monooxygenases, members of Group B keep NADPH/ $NADP^+$ bound throughout the catalytic cycle, stabilize their C4a-(hydro)peroxyflavin intermediates whilst the substrate usually binds after the peroxyflavin adduct is formed [11]. Among Group B monooxygenases that have been well characterized is Siderophore A (EC 1.14.13.196) from *Aspergillus fumigatus (Af* SidA*)*. This enzyme catalyzes the hydroxylation of ornithine to N^5-hydroxyornithine, the first step in the

biosynthesis of hydroxamate-containing siderophores using NADPH and oxygen as substrate [2]. Detailed kinetic and structural studies of this enzyme revealed that the enzyme is highly specific for L-ornithine. Studies also showed that, SidA preferentially uses NADPH over NADH forming a C4a-hydroperoxyflavin, the hydroxylating species. Furthermore, the C4a-(hydro)peroxyflavin intermediate is observed when NADPH is used as an electron donor and its decay is facilitated by the binding of its substrate, L-ornithine [13, 14]. Crystal structure studies confirmed size exclusion data previously published that SidA is a homotetramer [13]. The crystal structure in complex with $NADP^+$ and ornithine or lysine highlighted the importance of $NADP^+$ for stabilization of the intermediate and the position of binding of ornithine adjacent to $NADP^+$(Figure 2A). These studies thus explained the substrate specificity of SidA, which like PvdA, another member of this class is specific for L-ornithine [14, 15]. Even though SidA can also hydroxylate lysine, crystal structural studies revealed similar binding geometry as ornithine, except for a shift of ~ $1A^o$, which can be explained by the differences in the side chains of ornithine and lysine (Figure 2B). These kinetic and structural studies established the specificity of SidA for ornithine in preference to lysine [11]

Group C monooxygenases, possess a TIM barell structure. Two enzymes amongst this group that have extensively been characterized are the bacterial luciferase (EC 1.14.14.3) enzyme and the alkane sulfonate monooxygenase (EC 1.14.14.5). In the bacterial luciferase system, NMR studies have been used to prove the formation of the C4a-hydroperoxyflavin [1]. Flavin transfer has recently been suggested for this system to be by free diffusion of the reduced FAD from the reductase to the monooxygenase component [16].

Tryptophan 7-halogenase remains the prototype in group F monooxygenases. The catalytic mechanism of this enzyme revealed the formation of flavin C4a-hydroperoxide, which reacts with chloride ion producing a powerful oxidant hypochlorous acid [17]. Crystal structural analysis suggests that the hypochlorous acid is guided to the binding site of the substrate that allows selective halogenation of its substrate, tryptophan [18].

(A) **(B)**

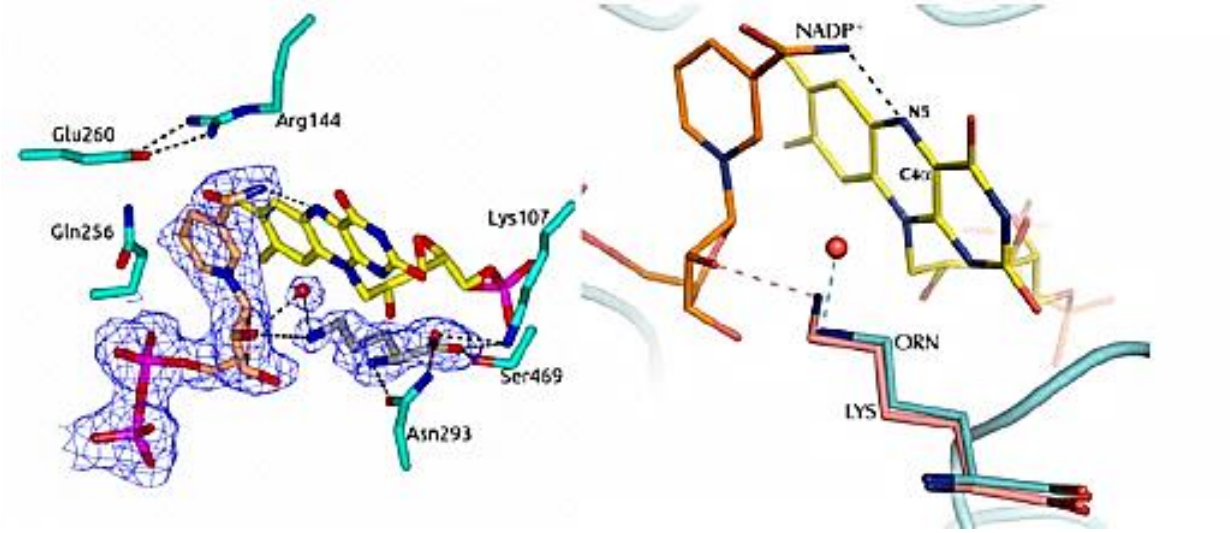

Figure 2. (A) Active site of *Af*SidA, a single component class B monooxygenase complexed to $NADP^+$(orange carbons), FAD (yellow carbons) and the substrate ornithine in (gray carbons). (B) The binding of ornithine (cyan carbons) compared with the binding of lysine (salmon carbons) [11].

1.4 Two-component monooxygenase systems

Two-component flavin-dependent enzymes catalyze a variety of oxidation-reduction reactions important in microbial biosynthesis of natural products, antibiotics and anti-tumor drugs, bioluminescence and desulfurization of sulfonated compounds [19]. These enzyme systems are composed of a reductase, which generates a reduced flavin that is transferred to a monooxygenase component that utilizes the reduced flavin to catalyze the hydroxylation of substrate as shown in scheme 1[20]. Two-component monooxygenases ensure the minimization of auto-oxidation or the production of reactive oxygen species such as H_2O_2 by efficient transfer mechanisms of the reduced flavin to the monooxygenase component since this reduced flavin is unstable and can react with oxygen [20]. Previous studies have shown that they partly overcome this problem through the reduced flavin normally having a higher affinity for the monooxygenase component than the reductase component (Table 2).

Two mechanisms employed by two-component monooxygenase systems, for reduced flavin transfer, that have been studied include; 1) free diffusion of the flavin from reductase to monooxygenase or 2) by protein-protein interactions between reductase and monooxygenase components. They can further be divided on their dependence for FMN or FAD. FAD-dependent enzymes include *p*-hydroxyphenylacetate hydroxylase (HpaA) [21-23], isobutylamine-N-hydroxylase (*vlmH)* [24, 25] and styrene monooxygenase (SMOA) [26, 27]. The mechanism of hydroxylation of their substrates is likely through the formation of a C4a-hydroperoxyflavin upon activation of reduced FAD by oxygen [19]. In general, two-component monooxygenases catalyze flavin reduction and oxidation on two-separate polypeptide units, a feature that clearly distinguishes them from single component flavin-dependent enzymes that catalyze flavin oxidation and reduction on a single polypeptide unit as shown in scheme1.

(A)

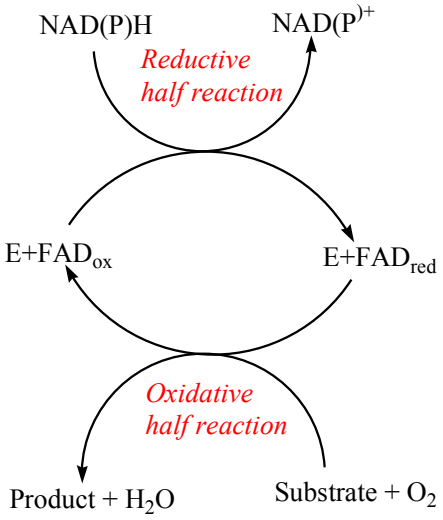

(B)

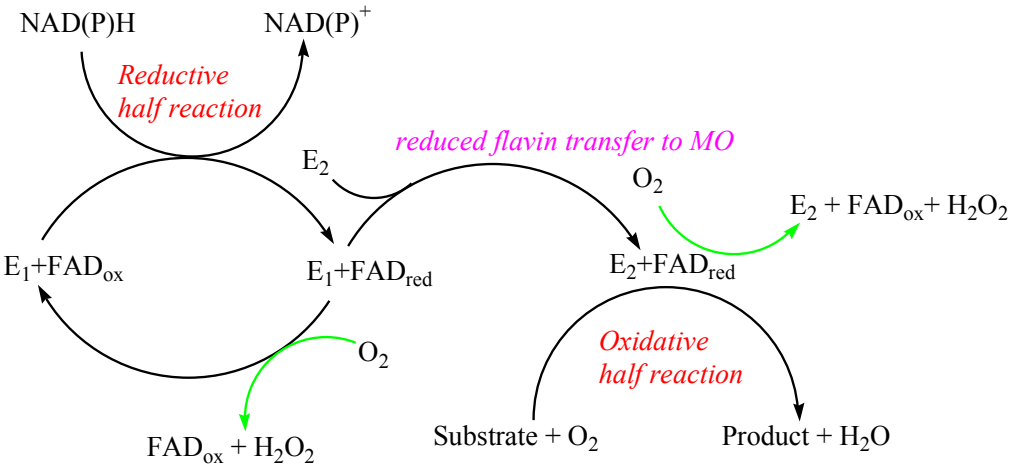

Scheme 1. Differences in reactions catalyzed by (A) single-component flavoproteins and (B) two-component flavoproteins. In these reactions, NAD (P)H serves as an electron donor to generate the reduced flavin in the reductive half reaction. The reduced enzyme reacts with oxygen and substrate to form the hydroxylated product in the oxidative half-reaction. (A) For single-component enzymes, the oxidized (FAD_{ox}) and reduced flavin (FAD_{red}) reside in the same active site of one protein unit. (B) In two-component monooxygenase systems, the generation of the reduced flavin usually by the small reductase component (E_1) is followed by its transfer to the second larger protein component, the monooxygenase, (MO or E_2). The green arrow shows the side reaction paths through which oxygen can react with free reduced flavin or E_2-bound reduced flavin to form hydrogen peroxide in the uncoupling path without hydroxylation.

TABLE 2

Dissociation constants (K_d) of the reduced flavin (Fl_{red}) and oxidized flavin (Fl_{ox}) for some two-component monooxygenases

Reductase	K_d of Fl_{red}	K_d of Fl_{ox}	Oxygenase	K_d of Fl_{red}	K_d of Fl_{ox}	Ref.
[a]ActVB/ µM	6.6	4.4	ActVA	0.39	19-26	[28]
[b]C_1-HPA/ µM	0.038	0.038	C_2-HPA	1.2	250	[29]
[c]HpaC/ µM	20	3	HpaA	2	250	[30]

[a] K_d range was approximated from absorbance and fluorescence spectroscopy measurements.
[b] Determination of K_d values was by ultracentrifugation techniques to determine bound versus free FAD
[c] Measurements were determined using fluorescence spectroscopy

1.5 Isobutylamine *N*-hydroxylase (IBAH)

Isobutylamine *N*-hydroxylase is an enzyme that catalyzes the oxidation of isobutylamine (IBA) to isobutylhydroxylamine (IBHA) in the presence of oxygen and a reduced flavin. The enzyme can be described as a member of group D flavin dependent monooxygenases [1]. In comparison to other *N*-hydroxylases, the reduced co-factor is supplied by a flavin reductase present in extracts of *S. viridifaciens*. Preliminary data involving characterization of the IBAH monooxygenase system revealed that IBAH utilized FAD and NADPH in preference to FMN, riboflavin and NADH [31]. Substrate specificity studies of the enzyme showed that IBA possesses the highest activity in comparison to other amine substrates tested [32]. The reductase component, flavin reductase has been identified as an NADPH oxidoreductase which was able to supply reduced flavin to the monooxygenase component for its catalytic activity [31]. No further characterization of this enzyme system has since been determined and there is no crystal structure available for this or other enzymes in this group of monooxygenases, making IBAH an attractive system to study.

1.5.1 IBAH in the valanimycin biosynthetic pathway

IBAH catalyzes the oxidation of IBA to IBHA in the valanimycin biosynthetic pathway of *Streptomyces viridifaciens.* Studies into the biosynthesis of valanimycin have shown that it is derived from L-serine and L-valine and that the valine is incorporated via the intermediacy of IBA to IBHA [33]. Valanimycin is an azoxy antibiotic that exhibits antibacterial activity and has been demonstrated to possess *in vitro* anti tumorigenic activity against cell cultures of mouse leukemia L1210, P388/S (duxorubicin sensitive) and P388/ADR (duxorobicin resistant) [34].

1.5.2 Reaction catalyzed by IBAH and FRED

Investigations on IBAH and FRED have established that the reaction catalyzed can be divided into a reductive half reaction in which flavin reductase generates the reduced flavin for the monooxygenase component IBAH that catalyzes the oxidation of IBA to IBHA using molecular oxygen [31]. FRED utilizes NADPH as a substrate in generating reduced flavin, which is transferred to IBAH for hydroxylation of its substrate (Scheme 2).

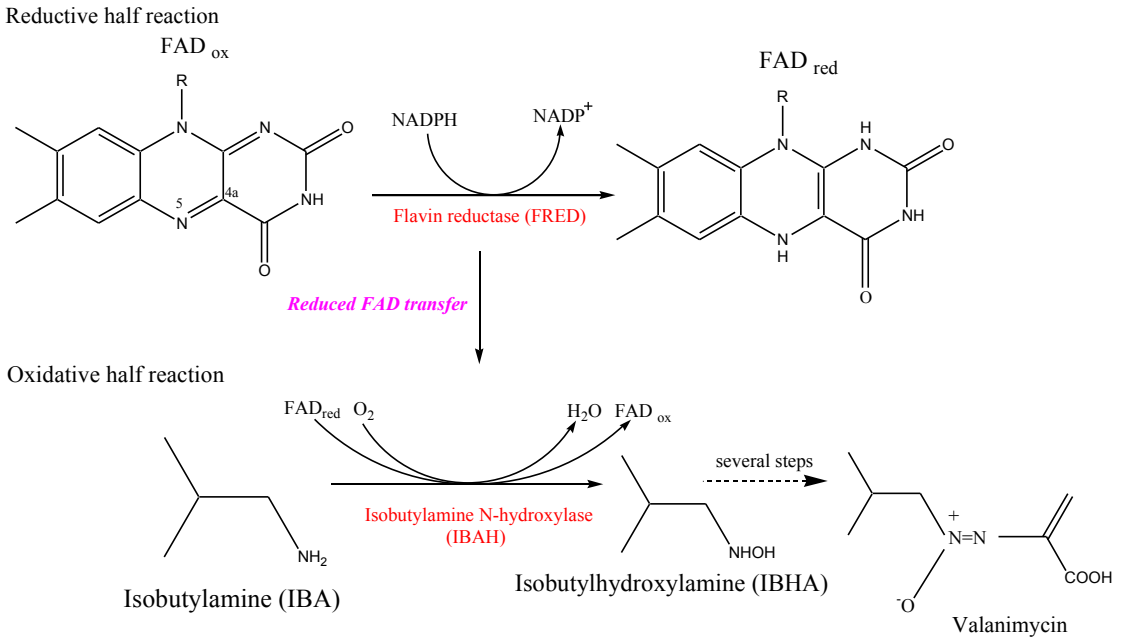

Scheme 2. The reaction catalyzed by isobutylamine *N*-hydroxylase and flavin reductase can be separated into reductive and oxidative half reactions. The reductive half reaction consists of a FRED-catalyzed oxidation of NADPH, which yields reduced FAD. In the oxidative half reaction, IBAH utilizes reduced FAD (FAD_{red}) and molecular oxygen as substrates to catalyze the hydroxylation of its substrate, isobutylamine (IBA) to isobutylhydroxylamine (IBHA).

1.6 Significance of project and aims

Preliminary studies by Parry and Li, (1997) into IBAH revealed successful expression and purification of both monooxygenase and reductase components. Kinetic data previously provided, highlighted the reaction mechanism but failed to establish a detailed catalytic mechanism for the IBAH monooxygenase system. Further kinetic characterization of this enzyme is therefore needed to establish a detailed catalytic and chemical mechanism. This work encompasses the expression, purification, steady state and pre-steady state characterization of this enzyme system. The end goal of proposing a kinetic mechanism will help in further elucidation of the role of the IBAH monooxygenase system. This study offers prospects of contributing to the depth of knowledge available in flavoenzymology for further understanding of the functions and mechanisms of flavin-dependent monooxygenases. The aims of this work are;

Aim1. Expression and purification of IBAH and FRED

Aim 2. Steady state kinetic characterization of FRED and IBAH

Aim 3. Pre-steady state kinetic characterization

CHAPTER 2: Materials and Methods

2.1 Materials

The synthetic gene encoding isobutylamine *N*-hydroxylase *(*IBAH) and Flavin reductase (FRED) from *Streptomyces viridifaciens* were obtained from Genscript (Piscataway, NJ). *E. coli* Turbo BL-21 DE3® chemically competent cells were from Invitrogen. Protein purification was carried out on an AKTA Prime Plus Fast Protein Liquid Chromatography (FPLC) (GE Healthcare). IBA was obtained from Sigma Aldrich. NADPH, buffers and salts were from Fisher Scientific. Tryptone and yeast extract used in preparation of Terrific Broth (TB) media were obtained from Fisher Scientific. The derivatization reaction was analyzed on an Ultraperformance Liquid Chromatography system (UPLC) (Waters, Milford, MA). HPLC separation was performed on an Agilent 1200 High Performance Liquid Chromatography (HPLC) system and a Phenomenex LUNA C18 (2) column was used. Rapid reaction kinetic experiments were performed on an Applied Photophysics SX20 stopped-flow spectrophotometer (Leatherhead, UK) installed in a Coy Glove Box (Grass Lake, MI).

2.2 Expression and purification of IBAH

The synthetic gene coding for IBAH was contained in pET15b, harboring an N-terminal His_6-tag. The gene was subsequently transformed into *E. coli* BL- 21 (DE3) cells and spread on LB plates supplemented with ampicillin (50 μg/mL). A single colony was inoculated into LB broth supplemented with ampicillin (50 μg/mL) and incubated overnight with shaking at 37 ºC. The seed culture was used in inoculation of six flasks containing ~ 1 L of Terrific broth supplemented with ampicillin (50 μg/mL), phosphate

buffer, succinic acid, $MgSO_4$, and 30X media containing 15% (w/v) lactose, 24% (v/v) glycerol and 0.45% (w/v) glucose for auto induction. Cultures were incubated at 37 ºC for ~ 5 h with agitation at 250 rpm until their optical density reading at 600 nm reached ~ 3.6. The temperature of the cultures was lowered to 18 ºC and left shaking overnight. Cell harvesting was carried out the next day and the cell pellets were stored at -80 ºC until downstream procedures were carried out. Cell pellets (40 g) were re-suspended in buffer A (25 mM HEPES, 5 mM imidazole, 300 mM NaCl and 15% glycerol, pH 7.5) and the mixture was incubated at 4 ºC for 45 min in the presence of 1 mM phenylmethanesulfonylfluoride (PMSF), DNase I, RNase and lysozyme (each at 25 μg/ml). All other steps were performed at 4 ºC. Cells were lysed by sonication using a Fisher Scientific Sonic Dismembrator Model 500 at 70% amplitude for 20 min (5 s pulse with 10 s delay) and the resulting extract was clarified by centrifugation (16, 500 × *g* for 1 h). The supernatant from this step was loaded at a flow rate of 3 mL/min onto 3 in-tandem 5 mL HisTrap crude columns (GE Healthcare) previously equilibrated with buffer A. The nickel column was then washed with buffer A followed by stepwise gradient elution using 150 mL each of 35 mM and 95 mM imidazole. Bound recombinant IBAH was eluted with 100% of buffer B (25 mM HEPES, 300 MM NaCl, 300 mM imidazole, 15% glycerol pH 7.5) using 300 mM imidazole at a flow rate of 2 mL/min. Fractions that contained IBAH were confirmed by analysis on a sodium dodecyl sulfate polyacrylamide (SDS-PAGE) gel. Fractions containing the protein were combined and dialyzed overnight against 2 liters of buffer C (25 mM HEPES, 150 mM NaCl, 15% glycerol pH – 7.5). The protein sample was then concentrated using a 30 kDa Amicon® Ultra Centrifugal filter membrane to about 15 mL volume. The final concentration of the protein sample was determined using the

Bradford assay. Generally, the final protein yield was 62.5 mg/L and the total protein was 150 mg representing 3.75 mg/g of purified protein per gram of wet cell paste. Aliquots were flash frozen in 20 μl drops in liquid nitrogen followed by storage at -80ºC.

2.3 Expression and purification of FRED

The synthetic gene coding for FRED was present in pET15b, containing an N-terminal His_6-tag. The gene was subsequently transformed into *E. coli* BL- 21 (DE3) cells and spread on LB plates supplemented with ampicillin (50 μg/mL). A single colony was inoculated into LB broth supplemented with ampicillin (50 μg/mL) and incubated overnight with shaking at 37 ºC. The seed culture was used in inoculation of six flasks containing ~ 1 L of Terrific broth supplemented with ampicillin (50 μg/mL), phosphate buffer, succinic acid, $MgSO_4$, and 30X media containing 15% (w/v) lactose, 24% (v/v) glycerol and 0.45% (w/v) glucose for auto induction. Cultures were incubated at 37 ºC for ~ 5 h with agitation at 250 rpm until their optical density reading at 600 nm reached ~ 3.6. The temperature of the cultures was lowered to 18 ºC and left shaking overnight at 250 rpm. Cell harvesting was carried out the next day and the cell pellets were stored at -80 ºC until downstream procedures were carried out. *E. coli* cells harboring the recombinant protein (30 g) were resuspended in buffer A (25 mM HEPES, 5 mM imidazole, 300 mM NaCl and 15% glycerol pH 7.5) at 4 ºC. Subsequent steps of the purification process were performed at room temperature. Cell lysis was achieved via sonication using 70% amplitude and the resulting extract was clarified by centrifugation (16, 500 $\times g$ for 1 h 15 min). The supernatant obtained was loaded at a flow rate of 2 mL/min onto 4 in-tandem 5 mL HisTrap crude columns (GE Healthcare) previously equilibrated with buffer A.

Various concentrations of buffer B; 35 mM, 65 mM and 95 mM imidazole, each 150 mL in a stepwise gradient elution were used to wash the Nickel column to remove contaminants after which the protein of interest was then eluted using 100% of buffer B (25 mM HEPES, 300 mM NaCl, 300 mM imidazole, 15% glycerol pH 7.5) at a 300 mM imidazole concentration. SDS-PAGE gel was used to analyze samples from various steps of the purification. Samples containing the protein were combined and dialyzed in buffer C (25 mM HEPES, 300 mM NaCl, 10% glycerol) for 2 h. Generally 49 mg/L of protein yield was obtained from 127.5 mg of protein, which represents 4.25 mg/g of purified protein per gram of cell paste. The protein sample was flash frozen in 20 μl drops in liquid nitrogen and stored at -80ºC.

2.4 NADPH oxidase activity

The activity of the reductase component was detected by a spectrophotometric assay measuring the decrease in absorbance of NADPH at 340 nm. (ε= 6.27 mM cm^{-1}) in 100 mM sodium phosphate buffer pH 7.5. The standard assay (1 mL) contained 10 μM FAD and was initiated by addition of 50 nM FRED. In assays where NADPH concentration was varied in the range 5-200 μM, 10 μM FAD was used. In assays where FAD concentration was varied 1-30 μM, 150 μM NADPH was used. Initial rates of reaction were recorded and plotted as a function of varying NADPH and FAD concentrations.

2.5 Flavin binding assay

The binding of FAD to flavin reductase was determined by monitoring the changes in flavin fluorescence at 526 nm (excitation at 450 nm) on a SpectraMax M5e plate reader (Molecular Devices, Sunnyvale, CA). The reaction was carried out in 50 mM Tris HCl

buffer, pH -7.0. The reaction mix consisted of 10 μM FAD with varying concentrations of FRED 0.2 – 70 μM. The reaction was prepared at a final volume of 25 μL and the plate was read using an instrument cut off at 455 nm. The affinity of FAD for FRED was determined by measuring the K_D value obtained by fitting the data to Michaelis Menten equation.

2.6 UPLC analyses of IBA consumption and IBHA production

The hydroxylation of IBA was monitored by ultraperformance liquid chromatography. The hydroxylation activity was monitored by mixing in a final volume of 100 μl, (20 μM IBAH, 0.5 μM FRED, 2 mM NADPH and 10 μM FAD and 0.5 mM IBA) in Tris HCl buffer pH 8.0. The reaction was quenched at 0, 5, 10, 30 and 60 min with 200 μl of 100% acetonitrile solution after which the reaction mixture was centrifuged to obtain the supernatant. The supernatant (100 μL) was withdrawn and mixed with 25 μL of 200 mM borate, pH 8.0. To derivatize the substrate IBA, 3.4 μL of FMOC (150 mM) prepared in 100% acetonitrile solution. The derivatization reagent, FMOC-Cl which reacts with primary amines was used in generating derivatives of IBA and IBHA which allowed monitoring at 263 nm, since the adducts formed produce absorbance at this wavelength. This was followed by incubation for 5 min at room temperature. Excess FMOC-Cl was removed by addition of 158 μL of 1-aminoadamantane (53 mM) and the reaction was then incubated at room temperature for an additional 15 min. An aliquot of 50 μL was withdrawn for UPLC analysis. This was achieved by loading 2 μL onto a C18 AcQuity column (2.1 x 100 mM) equilibrated in 70% eluent A (0.1 % trifluoroacetic acid in water) at 1 mL/min. The samples were eluted with a linear gradient from 40 - 100% buffer B

(0.1% trifluoroacetic acid in acetonitrile) at 1 mL/min, with monitoring of elution peaks at 263 nm.

2.7 HPLC ESI-MS analyses of FMOC Derivatives of IBHA and IBA

To analyze the incorporation of oxygen into the substrate IBA, reaction mixtures, were prepared as FMOC derivatives, as this permitted HPLC analysis using absorbance detection methods. Mass spectrometry was used to confirm the identity of the LC peaks observed. An HPLC column 250 x 4.6 mm 5 micron was utilized for the separation. The eluent A was water with 0.1% formic acid whilst eluent B was acetonitrile with 0.1% formic acid. The reaction consisted of 100 μL of 50 mM Tris HCl buffer pH – 8.0 containing (20 μM IBAH, 0.5 μM FRED, 2mM NADPH, 10 μM FAD and 1mM IBA) and stopped with 30% acetonitrile solution. The derivatization reaction with FMOC-Cl was carried out as described above. Reactions were analyzed using a flow rate of 1 mL/ min. The samples were eluted with a linear gradient of 0 -100% of eluent B. Column effluent was conducted via PEEK tubing first into a diode array detector, which measured the absorbance from 200-600 nm, and then into the Turboionspray source of an AB Sciex 3200 Qtrap mass spectrometer. Positive ions were detected over a mass range of 50-600 Da (at a rate of 1000 Da/sec) in the "enhanced" mode that is using the linear ion trap portion of the mass spectrometer.

2.8 Product formation Assay

To quantify the amount of hydroxylated IBA or product formed, a modified version of Csaky's iodine oxidation assay was used [35]. The standard reaction volume, 100 μL was performed in 100 mM sodium phosphate buffer pH 7.5, 25 ^{o}C. The reaction mix consisted of 50 nM FRED, 10 μM FAD and was initiated upon addition of 2 μM

IBAH. The reaction was incubated at 30 ºC for 30 min after which it was quenched with 2N perchloric acid. For each concentration of IBA/NADPH, 47.5 μL of the terminated reaction was transferred into a 1.5 mL eppendorf tube, and neutralized by the addition of 47.5 μL of 10% (w/v) sodium acetate solution. Subsequently, 47.5 μL of sulfanilic acid and 19 μL of 0.5% iodine solution were added. The mixtures were incubated at room temperature for 15 min. After this step, 19 μL of 0.1 N sodium thiosulfate solution was added to remove excess iodine. The color development reaction involved addition of 19 μL of 0.6% (w/v) α-naphthylamine in 30% (v/v) acetic acid followed by 45 min of incubation with shaking. The amount of hydroxylated IBA formed was measured at 562 nm on a Spectra M5e plate reader (Molecular devices). The amount of hydroxylated IBA formed from the reactions were determined using a standard curve previously prepared from hydroxylamine hydrochloride.

2.9 Oxygen consumption assay

The oxygen consumption activity was monitored by measuring the rate of oxygen consumption in a Hansatech oxygen monitoring system (Norfolk, England). The reaction was initiated upon addition of 1 mM NADPH to a final volume of 1 mL of 100 mM sodium phosphate buffer, pH 7.5. The reaction consisted of 10 μM FAD, 2 μM IBAH and 50 nM FRED. Substrate concentrations (IBA and NADPH) were varied from 0.025 – 5 mM. In assays where IBA was varied, 1 mM NADPH was used whilst 5 mM IBA was used where NADPH concentrations were varied.

Rapid reaction kinetics was carried out at 25 ºC using an SX-20 stopped-flow spectrophotometer (Applied Photophysics, Leatherhead, UK) installed in an anaerobic glove box. All solutions were prepared in anaerobic 100 mM sodium phosphate buffer, pH

7.5. The buffer, 200 mL volume was made anaerobic by repeated cycles of vacuum (15 min) and flushing with O_2-free argon for 5 h at room temperature, followed by overnight incubation in the glove box. The enzyme was made anaerobic prior to the experimental procedure by flushing with O_2-free argon and vacuum (15 min) for 90 min. The stopped flow apparatus was made anaerobic by an overnight incubation with oxygen scrubbing solution containing 100 mM glucose and 0.1 mg/mL glucose oxidase in 100 mM sodium acetate buffer pH 5.0.

2.10 Flavin reduction

The reduction kinetics of FAD bound to FRED, the reductase component was monitored using the single mode in the stopped flow using the reductants NADPH and NADH, in the presence and absence of substrate IBA. The reaction mixtures contained 10 μM FRED-FAD and varied concentrations of NADPH or NADH (0.05 - 4 mM). The FRED-FAD mixture (10 μM after mixing) was mixed with various concentrations of NADPH/ NADH 0.05 - 4 mM (final concentrations after mixing). Spectra for reduction was recorded by observing full reduction of FAD due to the decrease in absorbance at 450 nm. Measurements were recorded on a logarithmic scale in duplicates. The observed rate constants at various reductant concentrations were determined using the program KaleidaGraph (Synergy software, Reading, PA) by fitting the data to a single exponential decay equation. Dependence of the rate constants for the observed phases of the reaction was plotted against varying concentrations of NADPH/NADH and the data fitted to the equation 5, to yield the K_D and k_{red} of the reduction process.

2.11 Flavin reduction in the presence of substrate IBA

To determine if the substrate IBA had an effect on the kinetics of flavin reduction using NADPH, having confirmed this co-enzyme as a substrate for FRED, the reaction was carried out with 10 μM FRED-FAD mixed with 1 mM IBA (all final concentrations) and reacted with NADPH (0.05 - 4 mM). The substrate, 10 mM was prepared in 100 mM sodium phosphate buffer pH 7.5, containing glucose and glucose oxidase and left stirring overnight in the glove box. The FRED-FAD mixture 20 μM (initial concentration) was mixed with 2 mM IBA (initial concentration). Upon mixing, the final concentrations of FRED-FAD and IBA respectively were 10 μM and 1 mM. This mixture was reacted with NADPH 0.05 - 4 mM (concentration after mixing) and flavin reduction was monitored by observing a decrease in absorbance at 450 nm until full reduction was observed. Spectral measurements were obtained in duplicate and similar data analysis was performed as previously described in the absence of substrate to yield the rate of reduction under these assay conditions.

2.12 Flavin re-oxidation in the absence of monooxygenase component IBAH

Flavin re-oxidation was monitored in the absence of monooxygenase having observed that the reductase component alone possesses oxidase activity. The re-oxidation was carried out in the sequential double mixing mode on the stopped flow. The final concentrations of was 5.5 μM FAD-FRED after mixing and 5.5 μM NADPH (concentration after mixing) in 60 s to ensure complete reduction of the FAD with no NADPH in excess. In the second step, the completely reduced FAD was reacted with various concentrations of molecular oxygen (100 – 600 μM after mixing). The re-oxidation of FAD was monitored by observing the increase in absorbance at 450 nm until full re-oxidation was achieved. Stock

aerobic buffer was prepared by bubbling 100 mM sodium phosphate buffer for 30 min with 100% oxygen, and the subsequent concentrations were prepared by mixing with the required volume of anaerobic buffer. Data was fit to equation 6 and the observed k_{obs} values were plotted as a function of varying oxygen concentrations to obtain the rate of flavin re-oxidation.

2.13 Data analysis

Kinetic data were fit using Kaleidagraph (Synergy software, Reading, PA). Steady state data were fit to Michaelis-Menten equation (equation 1). Data that exhibited substrate inhibition kinetics were fit to equation 2 which yielded the K_M (Michaelis constant), k_{cat} (turnover number) and K_{is}, (substrate inhibition constant). Flavin fluorescence data were analyzed according to equation 3 to yield the K_D of FAD for FRED. For equation 3, F_{FRED} is the fluorescence at each FRED concentration N_{FRED}. In flavin reduction kinetics, the decrease in absorbance at 450 nm was fit to a single exponential decay equation (equation 4) and the resulting k_{obs} values were plotted as a function of NADPH concentrations. These data were fit to equation 5 to obtain the rate of reduction (k_{red}) and K_D values. Flavin re-oxidation data determined by observing the increase in absorbance at 450 nm was fit to a single exponential rise equation (Equation 6). The k_{obs} values obtained were plotted as a function of varying oxygen concentrations, which were then fit to a linear equation yielding the rate constant for flavin oxidation (k_{ox}).

$$v = \frac{V_{max}[S]}{K_M+[S]} \qquad \text{(Eq. 1)}$$

$$v = \frac{k_{cat}[S]}{K_M+[S]+[S^2]/K_{is}} \qquad \text{(Eq. 2)}$$

$$F = \frac{F_{FRED}[N_{FRED}]}{K_D + [N_{FRED}]} \quad \text{(Eq. 3)}$$

$$v = C + Ae^{-(k_{obs1}t)} \quad \text{(Eq. 4)}$$

$$k_{obs} = \frac{k_{red} \times [S]}{K_D + [S]} \quad \text{(Eq. 5)}$$

$$v = C + A(1 - e^{-(k_{obs}t)}) \quad \text{(Eq. 6)}$$

CHAPTER 3: Results

3.1 Expression of IBAH and FRED

The expression and purification of IBAH and FRED followed a generally successful pattern, with a few problems encountered in the initial purification stages of FRED. The genes encoding IBAH and FRED were synthesized and codon optimized in pET15b for expression in BL-21 DE3 cells (Figure 1). For expression, a total of about 16.7 g/L and 11.6 g/L of cell paste were obtained for IBAH and FRED respectively (Table 1).

3.2 Purification of IBAH and FRED

The purification process of IBAH yielded a soluble and stable protein with a yield of 62.5 mg/L of initial cell culture. The molecular weight of the protein was estimated to be ~ 40 kDa based on the SDS-PAGE analysis (Figure 2). The total protein yield was 150 mg, which represented 3.8 mg/g of protein per gram of cell paste (Table 1). In the FRED purification, a few problems of solubility of the FRED-purified protein were encountered in initial trials of the purification process. These problems were mitigated by the use of 15% glycerol in buffers, which greatly reduced the occurrence of aggregation problems initially encountered. A protein with a size of ~ 21.2 kDa, was observed from SDS-PAGE analysis (Figure 3). The protein concentration upon purification was 49 mg/L of initial cell culture. The total protein yield was 127.5 mg, which resulted in 4.3 mg/g of protein per gram of cell paste.

IBAH and FRED were both purified with no bound FAD as initials trial where FAD was added was washed off during the purification process. The polyhistidine tag bound to the recombinant proteins was not cleaved during the purification process. Protein

was flash frozen in 20 μl aliquots in 25 mM HEPES, 150 mM NaCl, 15% glycerol for IBAH and 25 mM HEPES, 300 mM NaCl, 15% glycerol for FRED and kept at -80 ºC, until downstream experiments were performed.

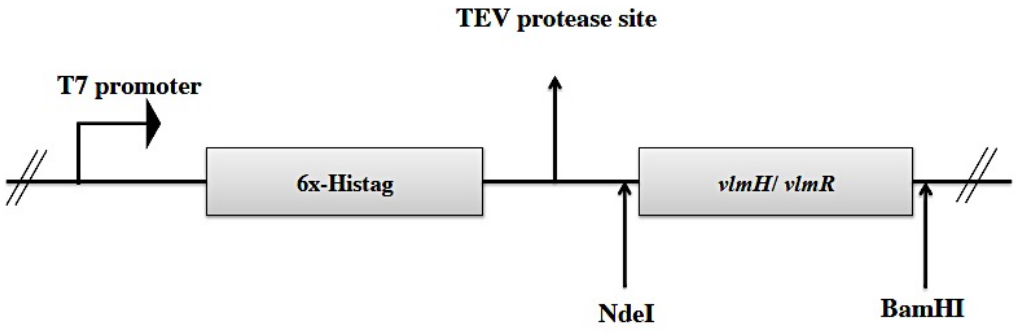

Figure 1. Plasmid construct map of pET15b for IBAH and FRED. The genes coding for IBAH and FRED, *vlm H* and *vlm R* respectively were synthesized and codon optimized for expression in *E. coli* cells BL-21 DE3 in the plasmid pET15b. The genes were cloned between the restriction sites *NdeI* and *BamHI*. In the plasmid, expression was under the control of the T7 promoter. The recombinant gene was synthesized in frame with a 6x-histidine tag site via a TEV cleavage site to allow for standardized IMAC purification.

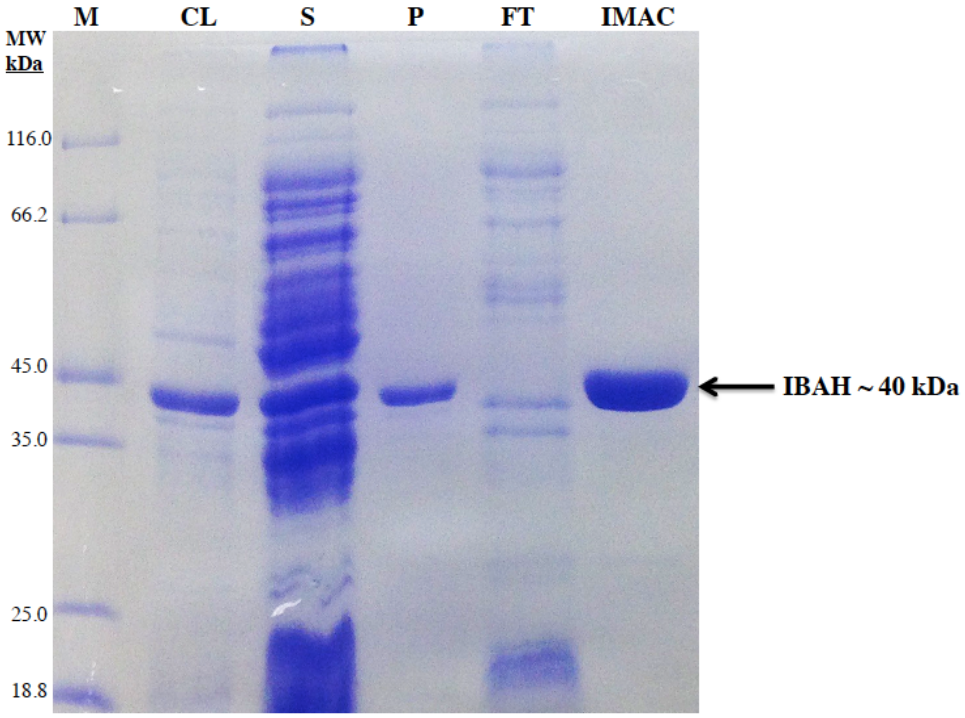

Figure 2. 12% SDS-PAGE gel summarizing purification of IBAH expressed as a fusion to a polyhistidine tag and purified using immobilized metal affinity chromatography (IMAC). **(M)** Marker; **(CL)** Cell lysate; **(S)** Supernatant; **(P)** Pellet; **(FT)** Flow through; **(IMAC)** IBAH eluted from the nickel column using 100% buffer B (25 mM HEPES, 300 mM NaCl, 300 mM imidazole, 15% glycerol)

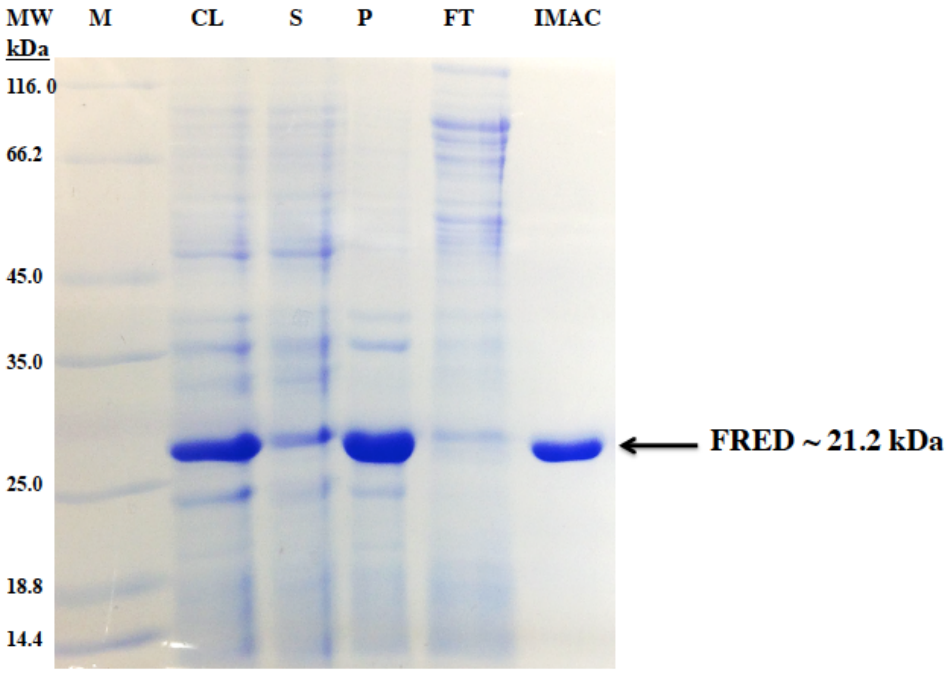

Figure 3. 12% SDS-PAGE gel summarizing purification of FRED expressed as a fusion to a polyhistidine tag and purified using immobilized metal affinity chromatography (IMAC). **(M)** Marker; **(CL)** Cell lysate; **(S)** Supernatant; **(P)** Pellet; **(FT)** Flow through; **(IMAC)** FRED eluted from the nickel column using 100% buffer B (25 mM HEPES, 300 mM NaCl, 300 mM imidazole, 15% glycerol)

TABLE 1
Summary of expression and purification of IBAH and FRED

Vector	Expressed-protein [a]	Expression medium	Cell pellets (g/L) [b]	Purified protein yield (mg/g)	Protein yield (mg/L)	Total protein (mg)
pET15b	His_6-IBAH	Terrific broth	16.7	3.8	62.5	150
pET15b	His_6-FRED	Terrific broth	11.6	4.3	49	127.5

[a] The construct for the expression vector is shown in Figure 1

[b] The weight of wet cells obtained and purified for 6 litres of culture after centrifugation was carried out as described in materials and methods section

3.3 NADPH oxidase activity

The oxidoreductase activity of the reductase component of the two-component monooxygenase system was monitored by measuring the decrease in absorbance at 340 nm of NADPH at either varying NADPH or FAD concentrations. The k_{cat} value calculated as a function of NADPH was 10.4 $\pm$ 0.5 s^{-1}. The K_M value of FRED for NADPH was 10.7 $\pm$ 2.2 μM. The K_M value for FAD was 2.5 $\pm$ 0.5 μM a 4-fold decrease in the K_M of NADPH, indicating a higher affinity of FRED for FAD than NADPH. The turnover number for FAD was 9.1 $\pm$ 0.5 s^{-1} (Table 2).

3.4 Flavin binding assay

The binding of FAD to FRED was measured by monitoring the fluorescence change of 10 μM FAD upon mixing with FRED (0.2 – 70 μM) in an opaque 96-well plate. The assay was performed to determine the dissociation constant of the FAD-FRED complex. The results show that the fluorescence spectrum of FAD increases markedly upon binding to the enzyme (Figure 5A). The increase in fluorescence increased with increasing enzyme concentration. The observed changes of FRED binding showed saturation at concentrations greater than 20 μM of FRED (Figure 5B). The excitation wavelength was 450 nm with fluorescence emission measured at 526 nm. The K_D of the FRED-FAD complex was determined using equation 3, by computing the fluorescence intensity at each FRED concentration, yielding a K_D value of 7.3 $\pm$ 1.3 μM (Figure 5B).

(A)

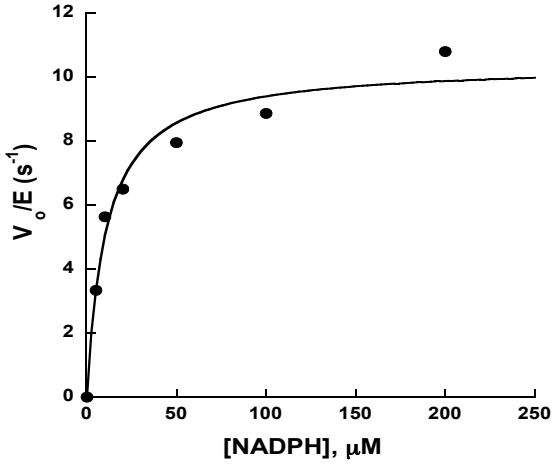

(B)

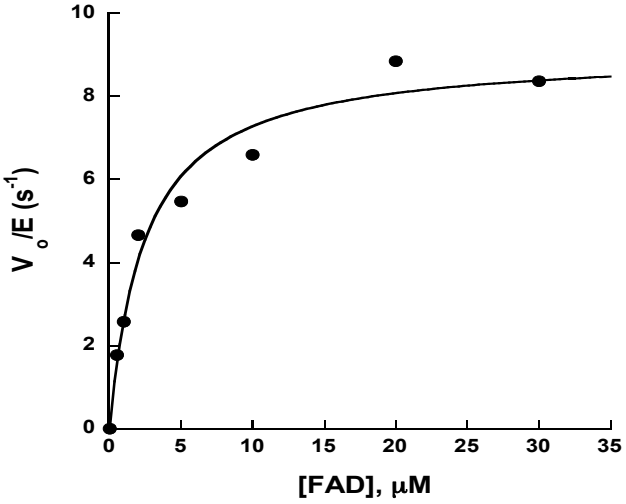

Figure 4. NADPH-oxidase activity of flavin reductase monitored by recording changes in absorbance at 340 nm. Initial rate of reaction plotted as a function of A) NADPH (5-200 μM) and B) FAD (0.5- 30 μM). The standard assay was performed in 100 mM sodium phosphate buffer pH 7.5 at 25 ^{o}C in the presence of 10 μM FAD where NADPH was varied and 150 μM NADPH where FAD was varied. The reaction was initiated upon addition of 50 nM FRED.

(A)

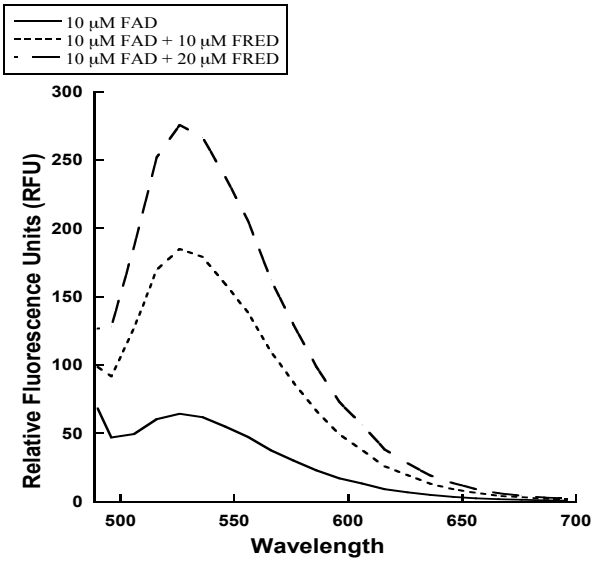

(B)

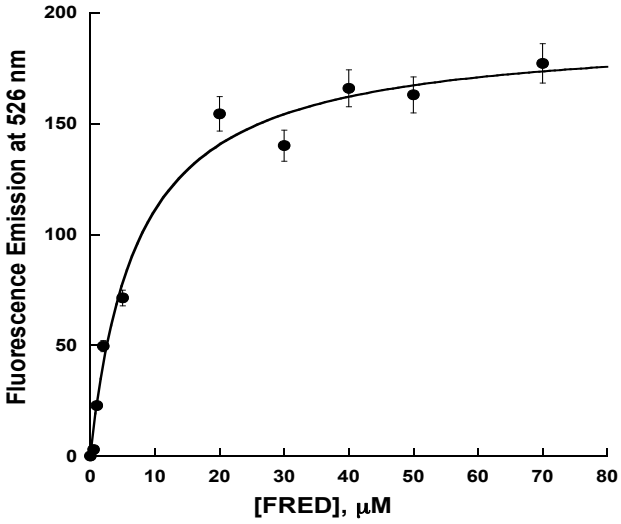

Figure 5. A) Effect of FRED on FAD fluorescence with excitation at 450 nm. B) Fluorescence intensity at 526 nm plotted as a function of FRED (0.2 – 70 μM). The standard reaction was performed in 50 mM Tris HCl buffer pH 8.0 at 25 ^{o}C with a cut-off of 455 nm on the plate reader.

TABLE 2

Kinetic data showing NADPH oxidase activity of FRED

Conditions were 100 mM sodium phosphate pH 7.5, 25 ^{o}C. The concentration of NADPH was 150 μM and of FAD was 10 μM.

Parameter	**NADPH**	**FAD**
k_{cat}, s^{-1}	10.4 ± 0.5	9.1 ± 0.5
K_M, μM	10.7 ± 2.2	2.5 ± 0.5
k_{cat}/K_M, $M^{-1}s^{-1}$	$(1 \pm 0.2) \times 10^6$	$(4 \pm 1) \times 10^6$

3.5 UPLC Derivatization of FMOC derivatives of IBHA and IBA

The derivatization reaction using FMOC-Cl was performed to assess the product formation activity of IBAH using the derivatization reagent fluorenylmethyloxycarbonyl chloride (FMOC-Cl). 1-aminoadamantane (ADAM) was added in the reaction to remove excess FMOC-Cl, which prevents the formation of FMOC-OH, which can interfere with the chromatographic procedure [36]. In a time-dependent manner, the product of IBA hydroxylation were observed to be increasing with IBA decreasing for reactions terminated at 0, 5, 10, 30 and 60 min (Figure 6B). Reverse phase chromatographic principles, allowed monitoring of the more polar product first [37]. Our results showed that IBHA eluted at ~ 1.8 min and the less polar adduct of IBA was eluted around 2.1 min. The peak observed for IBHA increased over time, whilst the substrate IBA decreased over time (Figure 6B).

3.6 HPLC Derivatization of FMOC derivatives of IBHA and IBA

The incorporation of an oxygen molecule into the substrate IBA was confirmed using mass spectrometry analysis. The derivatization reaction was carried out as previously described followed by separation by Reverse phase ultra-performance liquid chromatography (RP-UPLC) after which electrospray ionization mass spectrometry (ESI-MS) technique was used to fragment the samples to allow analysis of IBHA and IBA FMOC derivatives. The elution peaks were observed at 23.48 min and 27.92 min corresponding to IBHA and IBA respectively (Figure 7). Analysis of the IBHA peak when ionized using sodium or potassium yielded a m/z of 334.3 for the sodiated IBHA whilst the potassiated IBHA yielded a mass to charge ratio of 350.2 (Figure 8A). Further analysis of the IBA peak revealed a potassiated IBA peak of 334.4 and a

sodiated peak of 313.4 (Figure 8B). The analysis revealed that one molecule of oxygen is incorporated into IBA. The difference between the potassiated IBHA and IBA peaks gives a m/z difference of 16 which corresponds to one atom of oxygen (Table 3). The incorporation of oxygen can also be deduced for the sodiated IBHA and IBA peaks, thereby confirming that the product of the reaction of IBAH and FRED is a hydroxylated IBA (IBHA).

(A)

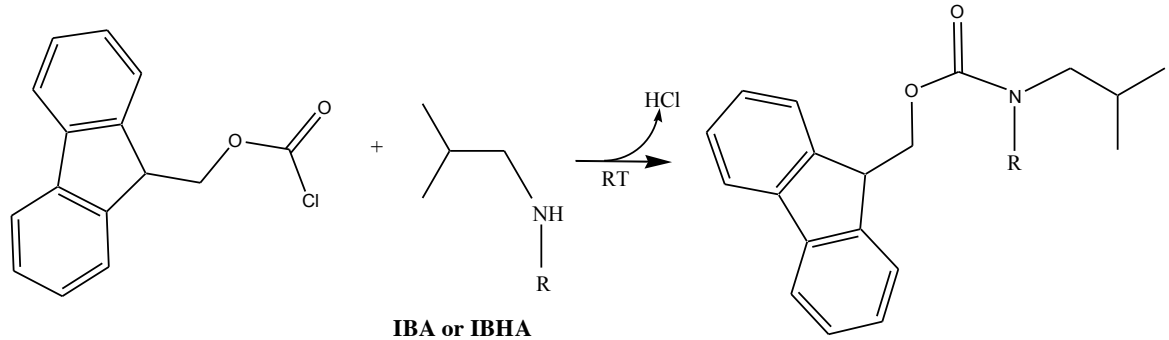

FMOC-Cl

IBA or IBHA (R can be H or OH)

Adduct formed between FMOC-Cl and IBA or IBHA

(B)

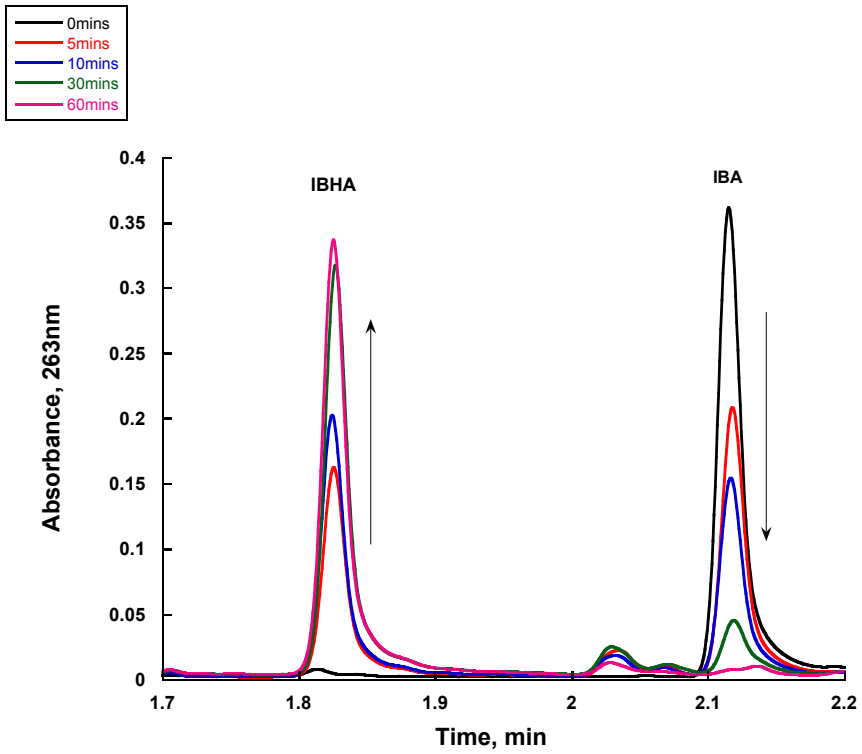

Figure 6. Production of hydroxylated isobutylamine, by IBAH and FRED. A) Scheme of the derivatization reaction of IBA or IBHA with FMOC-Cl. B) Traces of UPLC at 263 nm showing the elution of IBA and IBHA derivatized with FMOC-Cl. The time course of elution of the IBA peak decreases and the IBHA peak increases between 1 and 3 min.

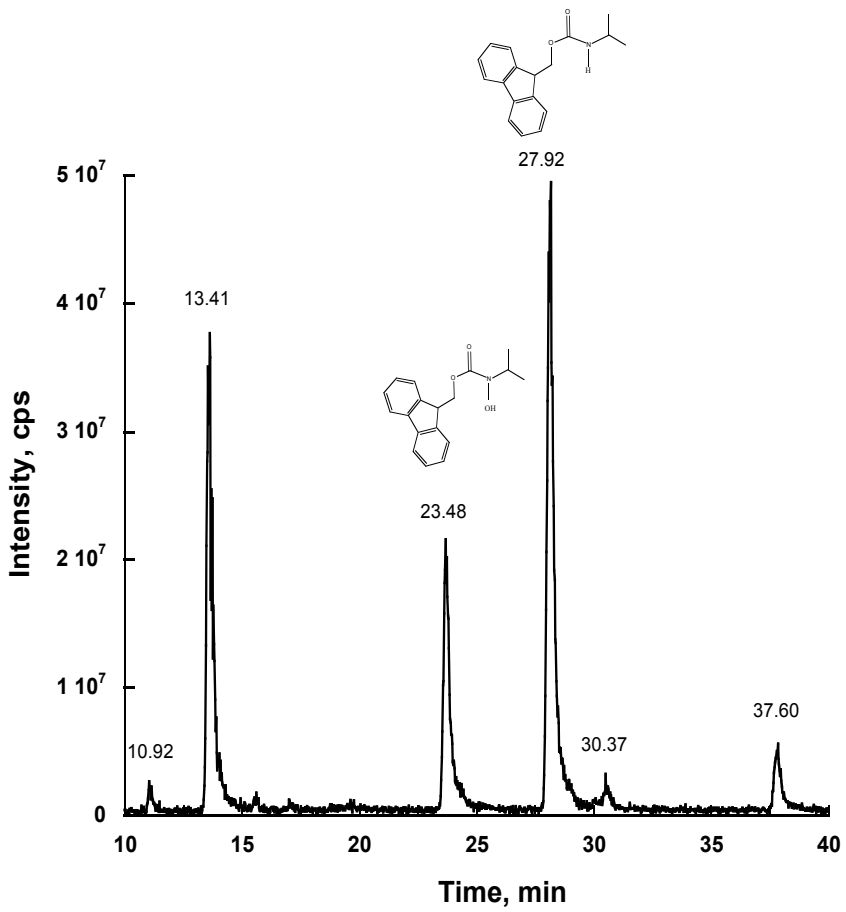

Figure 7. Extracted ion chromatogram from High Performance liquid chromatography analysis showing elution peaks of IBHA at 23. 48 min and IBA at 27.92 min. The peaks of IBHA and IBA show the structure of the product of the derivative with FMOC.

(A)

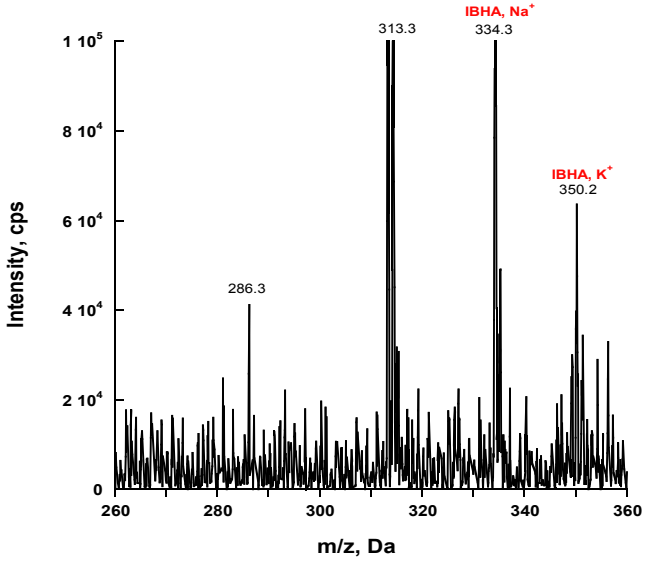

(B)

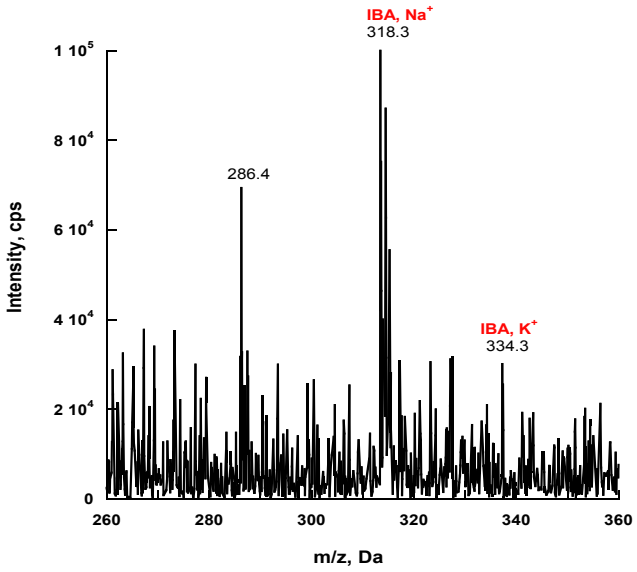

Figure 8. Graph of intensity plotted as a function of mass to charge ratio from LC-MS A) IBHA. The peaks 334.3 and 350.2 correspond to sodiated IBHA and potassiated IBHA respectively. B) IBA. The peaks 318.3 and 334.3 correspond to sodiated IBA and potassiated IBA respectively.

TABLE 3

Analysis of metabolic products of IBHA and IBA

	Metabolite[a]	Predicted masses (g/mol)	Observed m/z	Δm/z [b]	Predicted atom
Substrates	IBA-Na^+	317.36	318.4		
	IBA-K^+	334.47	334.3		
Products	IBHA-Na^+	334.13	334.3	16	Oxygen
	IBHA-K^+	350.24	350.2	16	Oxygen

[a] The ions of IBA(substrate) and IBHA(product) complexed with either Na^+ or K^+.

[b] The Δm/z was calculated by taking the difference between the peaks of the product and substrate for the potassiated or sodiated complex using the observed m/z values

3.7 Product formation Assay

To quantitate the amount of IBHA produced, a variation of the Csaky iodine oxidation assay was carried out [35]. The rate of formation of IBHA is dependent on substrate concentration as demonstrated in Figure 9. Substrate inhibition was observed in the presence of varying NADPH concentrations (Figure 9B). The k_{cat} value obtained in the presence of varying IBA was 0.012 ± 0.001 s^{-1} and for NADPH 0.016 ± 0.003 s^{-1}. The K_M values recorded were 200 ± 70 μM for IBA and 260 ± 90 μM for NADPH, indicating a higher affinity of IBAH for IBA than NADPH. The inhibition constant K_{is}, observed in the presence of varying NADPH concentrations was (1000 ± 400) μM, about a 5-fold higher value than the K_M of IBAH for NADPH. The catalytic efficiency of IBAH did not vary in the presence of either IBA or NADPH (Table 4).

3.8 Oxygen consumption activity

Kinetic data obtained for measurement of oxygen consumption by the monooxygenase component were plotted as a function of substrate concentration, with IBA saturating at 3 mM whilst NADPH was observed to have saturated at 5 mM (Figure 10). Data for the oxygen consumption activity is summarized in Table 4. In assays where IBA was varied, the background of oxygen consumption activity, in the absence of IBA was subtracted from the value obtained for each concentration of IBA. In assays where NADPH was varied, the oxygen consumption activity values obtained for each NADPH concentration in the absence of IBAH was subtracted from the values obtained in the presence of IBAH. These were done to ensure that only the activity of IBAH was measured under either assay conditions. The k_{cat} value obtained for IBA was 1.97 ± 0.06

s^{-1} and when NADPH was varied the k_{cat} was 1.91 ± 0.10 s^{-1}. The K_M of IBAH for NADPH was 2-fold higher than IBA, suggesting a higher affinity of IBAH for IBA. The catalytic efficiency of the enzyme was 2-fold increased for IBA 10,000.0 ± 2000 $M^{-1}s^{-1}$ as compared to NADPH 5000 ± 1000 $M^{-1}s^{-1}$. From table 4, it can be observed that, there is almost a complete uncoupling between oxygen consumption and substrate hydroxylation [38]. The degree of uncoupling was about 99% in the presence of either IBA or NADPH.

(A)

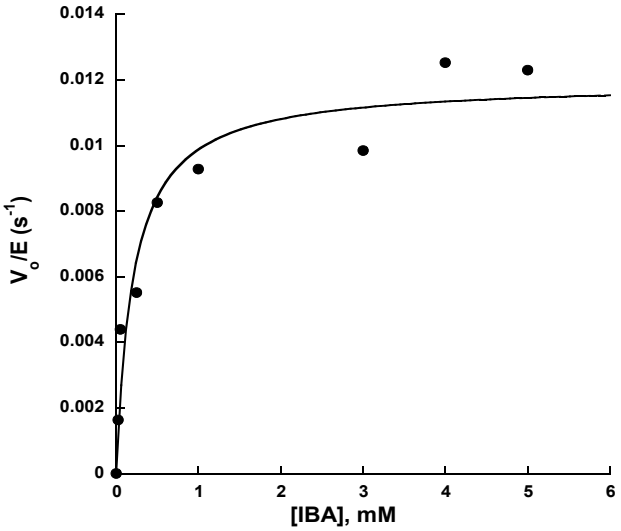

(B)

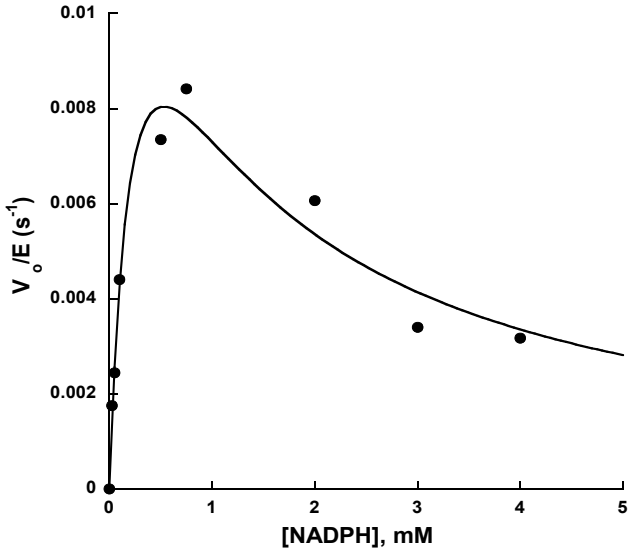

Figure 9. Product formation assay of IBAH and FRED. Rate of enzymatic reaction plotted as a function of IBA (0.025 – 5 mM) and B. NADPH (0.025 – 5 mM). The standard assay was performed in 100 mM sodium phosphate buffer pH 7.5 at 30 ^{o}C. 1 mM NADPH was used where NADPH was varied and 5 mM IBA was used where NADPH was varied. The assay was initiated upon addition of 2 μM IBAH in the presence of 50 nM FRED and 10 μM FAD.

(A)

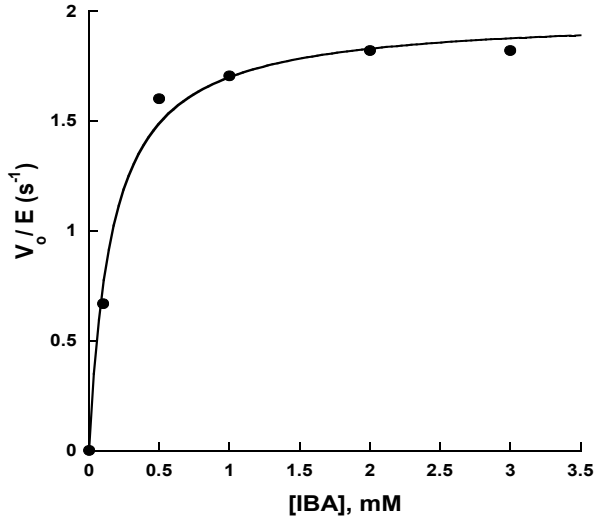

(B)

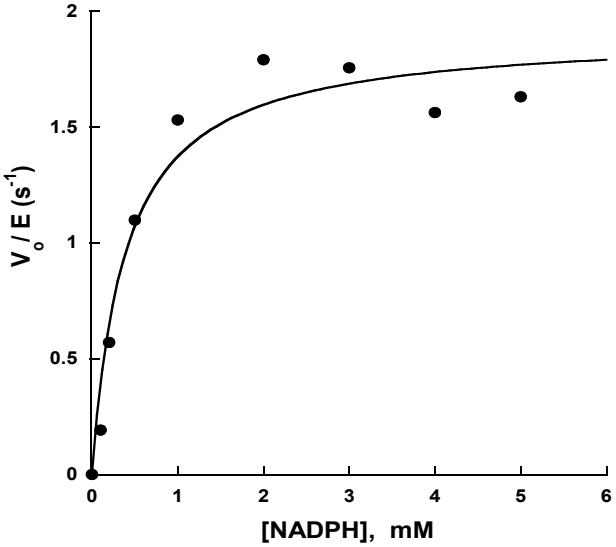

Figure 10. Rate of oxygen consumption as a function of A) IBA (0.05 – 3 mM) and B) NADPH (0.05 – 5 mM). The standard assay was performed in 100 mM sodium phosphate buffer pH 7.5 at 25 ^{o}C. In assays where NADPH was varied, 5 mM IBA was used whilst in assays where IBA was varied, 0.8 mM NADPH was used. The assay was initiated upon addition of 2 μM IBAH when NADPH was varied in the presence of 50 nM FRED and 10 μM FAD and 10 μM IBAH where IBA was varied.

TABLE 4

Steady state kinetic parameters for IBAH

Conditions were 100 mM sodium phosphate buffer pH 7.5, 25 ^{o}C for oxygen consumption assay. Uncoupling was calculated using the expression (1- $\frac{k_{cat(OH)}}{k_{cat(O2)}}$)×100, where $k_{cat\ (OH)}$ is the turnover number measured during hydroxylation of IBA and $k_{cat\ (O2)}$ is the turnover number measured during oxygen consumption. Conditions for product formation assay were 100 mM sodium phosphate buffer pH 7.5, 30 ^{o}C.

	Oxygen consumption		**Product formation**	
Parameter	**IBA**	**NADPH**	**IBA**	**NADPH**
k_{cat}, s^{-1}	1.97 ± 0.06	1.91 ± 0.10	0.012 ± 0.001	0.016 ± 0.003
K_M, μM	200 ± 30	400 ± 100	200 ± 70	260 ± 90
[a]K_{is}, μM	-	-	-	1000 ± 400
k_{cat}/K_M, $M^{-1}s^{-1}$	(1± 0.2) ×10^4	(5 ± 1)×10^3	60 ± 20	60 ± 20
Uncoupling %	99	99		

[a]Substrate inhibition was observed only in product formation assay where NADPH was varied.

3.9 Flavin reduction with NADPH in the absence of substrate

To monitor the reduction kinetics of FAD, FRED was mixed with various concentrations of anaerobic NADPH in the stopped flow in single-mixing mode, with monitoring of reactions by observing decreases in absorbance at 450 nm. The reduction as observed in figure 11A, was relatively rapid and was observed to be complete in about 3.59 s for 100 μM NADPH. The reduction of FAD bound to FRED observed in in the presence of NADPH followed uniphasic kinetics (Figure 11B). Further analysis of the reduction of FAD showed that the kinetics was dependent on NADPH concentrations (Figure 11) and approached limiting values of 8.57 ± 0.08 s^{-1} at the highest concentrations of NADPH > 2 mM. The rate of reduction, k_{red} was calculated as 10.0 ± 0.2 s^{-1} and the K_D of FRED for NADPH was 490 ± 40 μM (Table 5). The catalytic efficiency k_{red}/ K_D was 20,000 ± 200 $M^{-1}s^{-1}$. The data for computing the reduction rates was analyzed using equations 4 and 5.

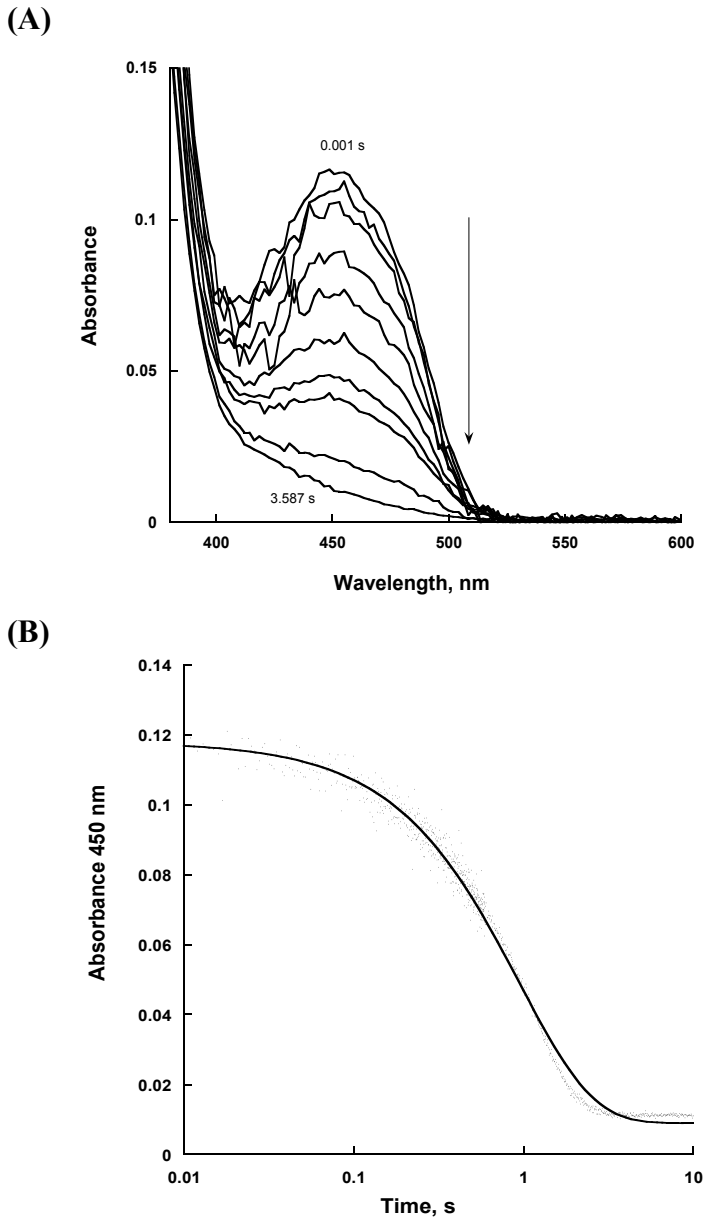

Figure 11. A) Absorbance changes observed at 450 nm using 100 μM NADPH. B) Changes in flavin absorbance at 450 nm at 100 μM NAPDH for flavin reduction. The changes in absorbance at 450 nm were fit to an exponential decay equation (solid line) to obtain the apparent k_{obs} values.

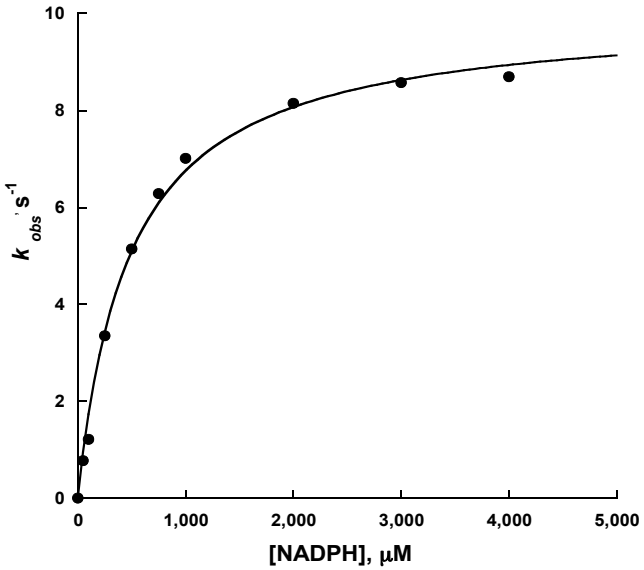

Figure 12. Flavin reduction monitored on the stopped-flow spectrophotometer using NADPH Dependence of the apparent k_{obs} values measured at each concentration of NADPH as a function of NADPH concentrations (0.05- 4 mM).

3.10 Flavin reduction with NADH in the absence of substrate

The reduction kinetics of FRED-FAD was assessed using NADH. The procedure was performed in the stopped-flow using various concentrations of anaerobic NADH while monitoring absorbance changes at 450 nm. Observing figure 13A shows that the reduction is completed in about 125 s. The reduction kinetics in the presence of NADH followed a uniphasic kinetic pattern as observed for NADPH (Figure 13B). Contrasting the characteristic dependence of NADPH on the reduction kinetics observed previously, when NADH was used as the electron donor for FRED, the apparent k_{obs} values increased linearly with respect to increasing NADH concentrations without reaching complete saturation levels in the presence of up to 4 mM NADH (Figure 14). The rate of reduction (k_{red}) was 0.35 ± 0.03 s^{-1} with a K_D of 3000 ± 500 μM (Table 5). The catalytic efficiency using NADH as an electron donor was measured as 100 $M^{-1}s^{-1}$ (Table 5). Data was analyzed using equations 4 and 5.

(A)

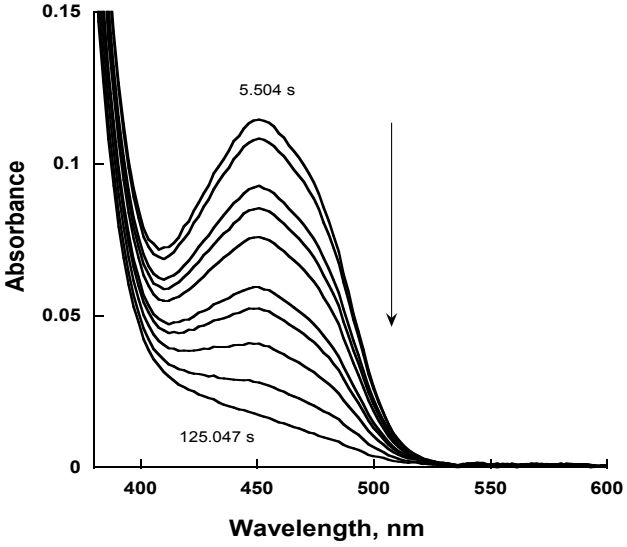

(B)

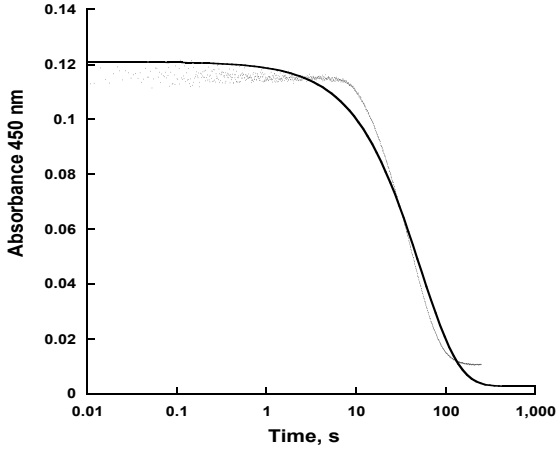

Figure 13. A) Absorbance changes observed at 450 nm using 100 μM NADH. B) Changes in flavin absorbance at 450 nm at 100 μM NADH for flavin reduction. The changes in absorbance at 450 nm were fit to an exponential decay equation to obtain the apparent k_{obs} values.

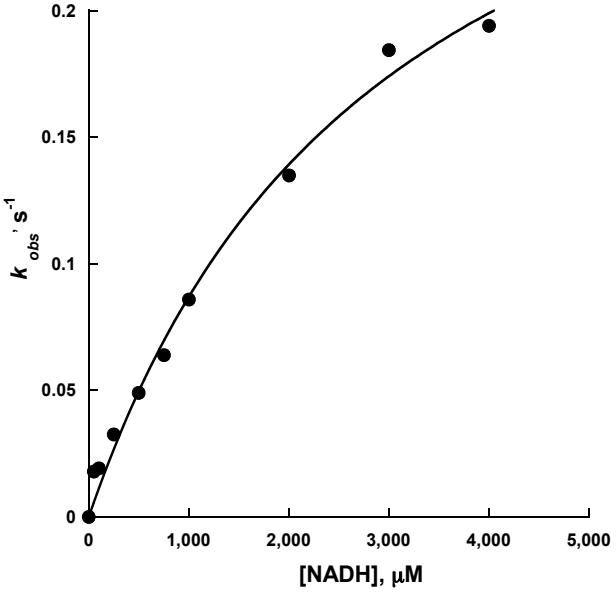

Figure 14. Flavin reduction monitored on the stopped-flow spectrophotometer using NADH Dependence of the apparent k_{obs} values measured at each concentration of NADH as a function of NADH concentrations (0.05- 4 mM).

3.11 Comparison of reduction rates of NADPH and NADH

The reduction kinetics when compared using NADPH or NADH, were observed to be altered significantly (Figure 15). About a 30-fold decrease in the rate of reduction, k_{red} was observed when NADH was used as an electron donor (Table 6). The dependence of reduction on NADPH reached limiting values at greater than 2 mM but this trend was not observed when NADH was used. The K_M in the presence of either NADPH or NADH was also affected, about 480 μM and 3000 μM respectively indicating a 6-fold decrease in the affinity of FRED for NADH. There was a robust catalytic efficiency of FRED when NADPH was used 20,000 ± 2000 $M^{-1}s^{-1}$ about a ~ 200-fold decrease compared to the efficiency of the enzyme in the presence of NADH.

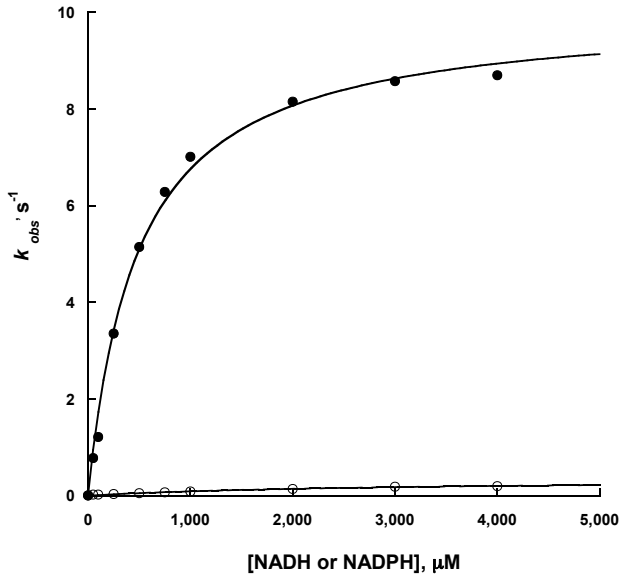

Figure 15. Flavin reduction monitored on the stopped flow. Apparent k_{obs} values as a function of NADPH (•) and NADH (○) (0.05- 4 mM). 10 μM of FAD was reacted with 10 μM FRED and mixed with varying concentrations of NADPH or NADH.

3.12 Flavin reduction with NADPH in the presence of substrate IBA

Observation from the reduction kinetics using either NADPH or NADH, showed NADPH as a preferred substrate for FRED. Hence the effect of substrate IBA was assessed using NADPH as the electron donor. Even though, theoretically IBA is not a substrate of FRED, stopped flow kinetics was used to assess the possibility of its effect on the reduction activity as seen in certain two-component systems [39]. Traces of reduction shows that complete reduction occurred in ~ 4.00 s (Figure 15A). The reduction of FAD in the presence of NADPH and 1 mM IBA followed a uniphasic kinetic behavior as observed in NADPH and NADH reduction kinetics in the absence of substrate (Figure 15B). The reduction activity was dependent on NADPH concentrations and reached limiting values at about 5.71 ± 0.06 s^{-1} at NADPH > 2 mM (Figure 16). The k_{red} of FRED in the presence of IBA was 6.6 ± 0.2 s^{-1} and the K_D was determined as 500 ± 50 μM. The catalytic efficiency of reduction by FRED was recorded as 13,000 ± 1000 $M^{-1}s^{-1}$ representing about a 1.5-fold decrease of reduction rate in the presence of substrate. The K_M values recorded in the presence and absence of substrate however were similar (Table 5). Since the catalytic efficiency was slightly decreased, to about 1.5 fold, this suggests that IBA does not affect the reduction kinetics of FRED.

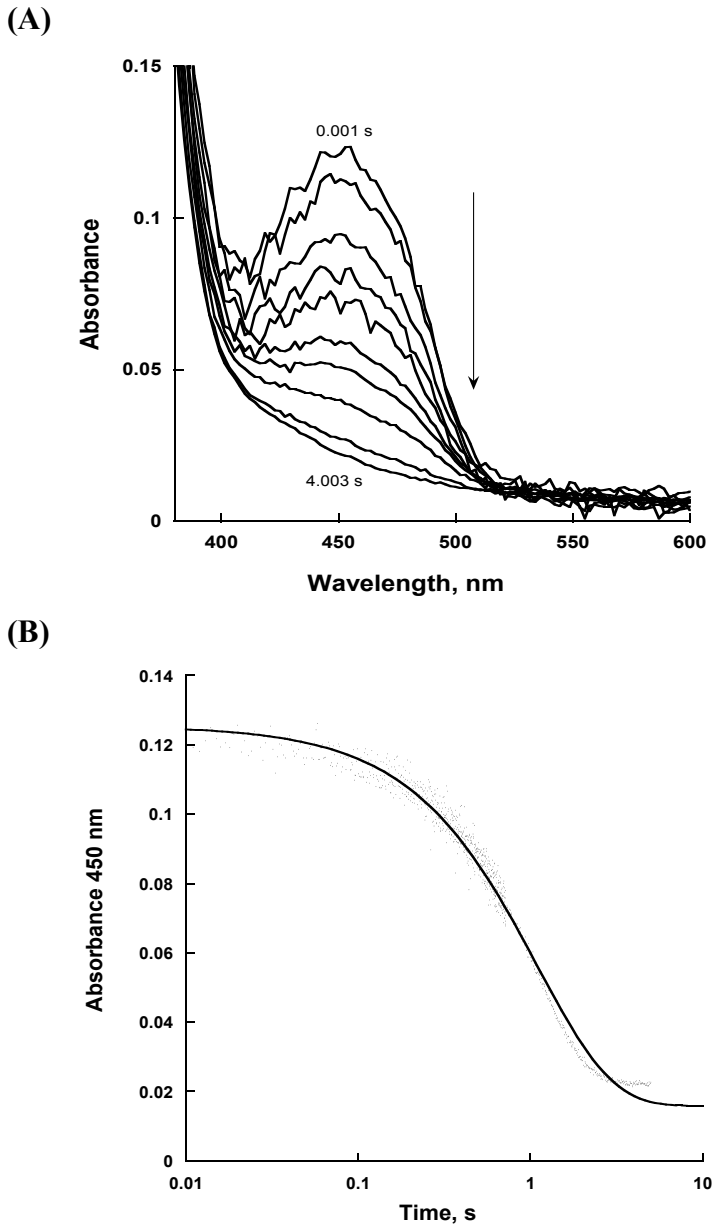

Figure 16. A) Absorbance changes observed at 450 nm using 100 μM NADPH in the presence of 1 mM IBA. B) Changes in flavin absorbance at 450 nm at 100 μM NADPH. The changes in absorbance at 450 nm were fit to an exponential decay equation to obtain the apparent k_{obs} values.

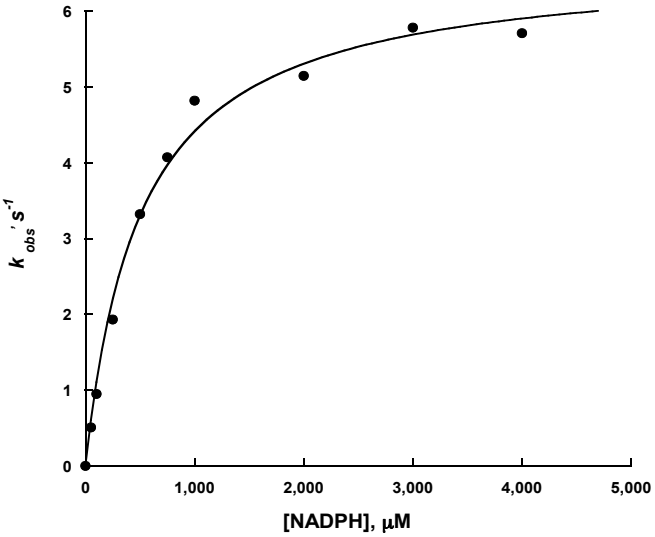

Figure 17. Flavin reduction monitored on the stopped-flow spectrophotometer using NADPH in the presence of 1 mM IBA. Dependence of the apparent k_{obs} values measured at each concentration of NADPH as a function of NADPH concentrations (0.05- 4 mM).

TABLE 5
Rapid reaction kinetic parameters for Flavin reductase activity
Conditions were 100 mM sodium phosphate buffer pH 7.5, 25 ^{o}C.

Parameter	NADPH	NADH	NADPH, IBA
k_{red}, s^{-1}	10.0 ± 0.2	0.30 ± 0.03	6.6 ± 0.2
K_D, μM	490 ± 40	3000 ± 500	500 ± 50
k_{red}/K_D, $M^{-1}s^{-1}$	20,000 ± 2000	100	13,000 ± 1000

3.13 Flavin re-oxidation in the absence of monooxygenase (IBAH)

The re-oxidation of $FADH_2$ was analyzed in the absence of the monooxygenase component, IBAH owing to the auto-oxidation activity exhibited by the reductase component of two-component systems [20]. The activity of oxidation was monitored in sequential double mixing mode on the stopped flow at 25 ^{o}C by mixing FAD-FRED (5.5 μM final concentration) and anaerobic 5.5 μM NADPH (final concentration) to ensure complete reduction of FAD before re-oxidation. Concentrations of oxygen tested were 100 – 600 μM. Traces showing absorbance changes at 450 nm show the re-oxidation occurring at a very fast rate and was completely re-oxidized in about 3.69 s for 200 μM O_2 (Figure 18A). Under the assay conditions tested, full re-oxidation of FAD was observed in a single phase (Figure 18B). The apparent k_{obs} values were computed for each concentration of O_2 and plotted against the respective varying O_2 concentrations (Fig 19). The rate of re-oxidation (k_{ox}) occurred at 4.79×10^{-9} $M^{-1}s^{-1}$ in the absence of monooxygenase, IBAH.

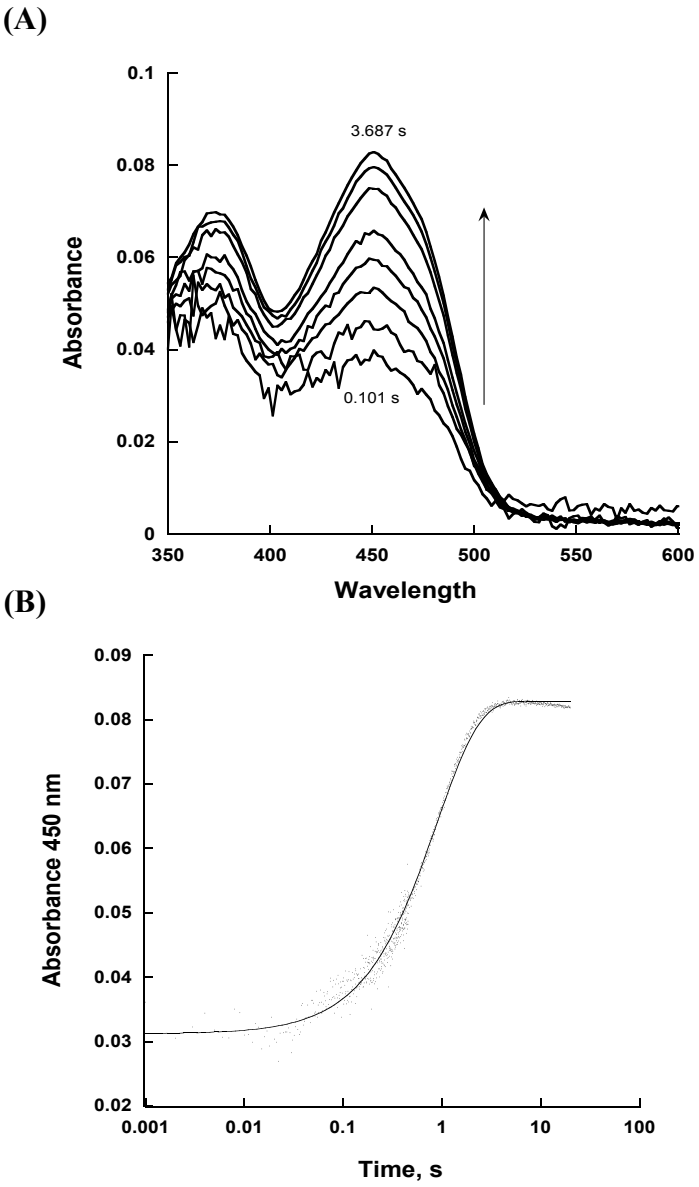

Figure 18. Flavin re-oxidation monitored on the stopped flow. A) Changes in absorbance at 450 nm as a function of time showing flavin re-oxidation for 200 μM O_2. B) Spectra changes of the reaction of reduced FRED-FAD with 200 μM O_2. The data was fit to an exponential rise equation

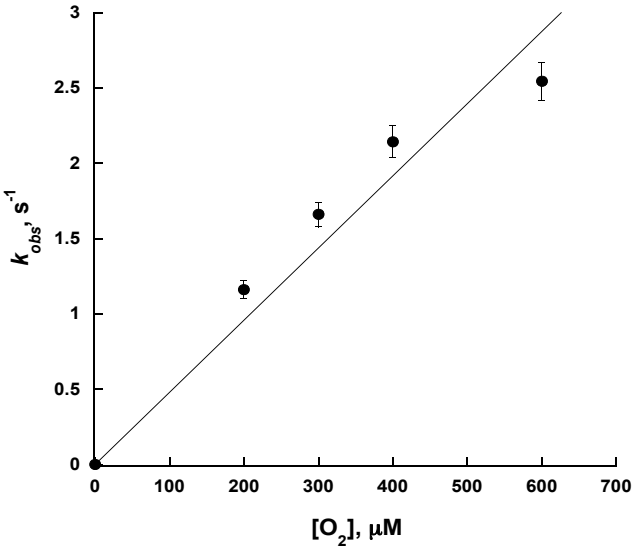

Figure 19. Apparent k_{obs} values plotted as a function of O_2 concentrations (100, 200, 300, 400, 500 and 600 μM O_2) in the absence of IBAH and substrate IBA. The k_{ox} for the re-oxidation in the absence of IBAH was 4.79×10^{-9} $M^{-1}s^{-1}$.

CHAPTER 4: Discussion

Infectious diseases remain the second leading cause of death worldwide with approximately 17 million deaths recorded annually due to bacterial infections [40]. The major public health burden posed as a result has been compounded by the increase in resistance to available antibiotics necessitating the discovery of new antimicrobials [41]. Manipulation of biosynthetic pathways of microorganisms involved in the synthesis of antibiotics offer exciting prospects into the discovery of new drugs to combat the menace of antibacterial drug resistance [42]. Studies into the mechanisms of enzymes that catalyze reactions in microbial biosynthetic pathways are essential in achieving the end goal of the synthesis of improved therapeutics for various bacterial infections.

Severe invasive infections caused by *Streptomyces species* have been rarely reported. Most of the cases reported, however, have occurred in immunocompromised individuals [43-46]. Characterization of the IBAH monooxygenase system, a class D two-component flavin dependent enzyme in the valanimycin biosynthetic pathway of *Streptomyces viridifaciens* presents attractive potential in drug development efforts towards infections caused by *Streptomyces species* as well as further understanding into mechanisms of flavin dependent enzymes.

The protocol developed for the expression and purification of IBAH and FRED included certain changes relative to the previously reported procedures [24, 31]. This includes the use of HEPES in the buffer system and the use of auto induction in expression of the recombinant proteins. Auto induction is based on the function of Lac operon regulatory elements in mixtures of glucose, glycerol and lactose under diauxic growth conditions. This method of induction has been reported to generally result in

higher cell densities and concentration of target proteins per volume of cell culture [47, 48]. Our results from the purification of IBAH showed relatively higher yield than those previously reported [25]. The use of auto-induction, may explain the high protein yield from the expression of IBAH. Even though the protein yield for FRED was relatively lower than previous reports, sufficient yields were obtained for the purpose of performing downstream experiments [31]. In the purification of FRED, the use of 15% glycerol in buffers for purification, led to considerable reduction in aggregation of the protein encountered in the initial phases of the process. Glycerol is known to prevent protein aggregation during refolding through preferential interaction with large patches of contiguous hydrophobicity where glycerol acts as an amphiphilic interface between the hydrophobic surface of proteins and the polar solvent [49].

In order to analyze the catalytic activity of FRED, an NADPH oxidase activity assay was carried out with saturating concentrations of substrates. The results show that FRED was capable of oxidizing NADPH in a substrate-concentration dependent manner. There was a 4-fold increase in the catalytic efficiency of FAD over NADPH due to the increased affinity of FRED for FAD over NADPH.

Fluorimetric titrations of FAD-FRED resulted in the measurement of the dissociation constant of FAD for FRED. The effect of FRED on the enhanced fluorescent intensity of FAD is consistent with previously published data [31]. The fluorescence of FAD has been shown to quench upon protein binding in the reductase component of some two-component systems [39, 50]. Our results show a contrasting effect where the fluorescence intensity is increased upon enzyme binding. The low sequence identity between FRED and its associated proteins including the reductase component of the two-

component system in *Acinetobacter baumannii* C_1-HPA, a class D monooxygenase may account for the differences in flavin dynamics exhibited upon enzyme binding (~ 21% sequence identity based on BLAST analysis). The increase in the intensity of the emission spectrum of the FAD as previously suggested may be due to movement of the adenine ring of the FAD away from the isoalloxazine ring since studies have shown that the stacking between these two rings quenches the fluorescence of free FAD [31, 51].

To quantify the IBHA generated, after confirmation of product formation, our results show the dependence of substrate concentration on the activity of IBAH. Lack of available information on quantification of hydroxylated product, as done in this work for two-component monooxygenases present challenges in comparing the data obtained with other systems. We further explored the activity of IBAH by measurement of oxygen consumption to assess the oxidation activity of the monooxygenase component. Since the oxidase activity of the reductase component has been established from characterization data from this work, the background of oxidase activity was subtracted from measurements involving the two proteins to ensure that, the resulting activity was due to the monooxygenase component. Comparison of the rates of oxygen consumption and product formation show a high degree of uncoupling of the IBAH monooxygenase system. The high level of uncoupling may be due to the production of reactive oxygen species as a result of oxidase activity as suggested in studies involving pyrole-2-carboxylate monooxygenase [52]. This pronounced uncoupling effect suggests that a large amount of the oxygen consumed by the IBAH monooxygenase system results in the formation of hydrogen peroxide without hydroxylation of substrate.

To gain further insight into the reductive half activity of FRED, the kinetics of FAD reduction was determined using rapid reaction kinetic. Our results indicate that the reduction occurs in single phase and is dependent on NADPH and NADH concentrations. The reduction in the presence of NADPH was 30-fold faster than NADH, and the affinity of FRED for NADPH is higher than NADH. The negative charge on the nucleotide (NADPH) appears to be important for the catalytic activity of FRED. Even though previous investigations established the preference of FRED for NADPH, our results are not comparable to the kinetic data reported but support their conclusions about the substrate preference of FRED for NADPH. [31].

In monitoring the reduction activity of FRED in the presence of substrate, IBA our results indicate traces of monophasic reduction of FAD as observed in reduction involving NADPH and NADH in the absence of substrate. The rate of reaction is decreased ~1.5-fold and the affinities of FRED for NADPH in the presence and absence of IBA, were not significantly altered. Detailed kinetic studies involving the reductase component of the *p*-hydroxyphenylacetate–hydroxylase (HPAH), of *Acenitobacter baumanii*, C_1-HPA revealed that the substrate, HPA though not a natural substrate of the reductase component, served as a substrate effector for the reduction activity. In the absence of substrate, the reduction was biphasic. In the presence of substrate HPA, the biphasic kinetic behavior was abolished, occurring in a single phase and was 30-fold faster and the affinity of the enzyme for NADH was stimulated ~80-fold [39]. Our results suggest a different mechanism for FRED; a monophasic reduction pattern that is NADPH dependent. IBA does not appear to be a substrate effector for the reduction activity. It can be suggested that, FRED may not exist as a mixture of isoforms as seen in the C_1-HPA

system. Even though FRED and C_1-HPA systems are both reductase components of class D monooxygenases, differences in their substrate specificities, reaction temperatures for the reduction activity and their low sequence identity could account for the differences observed in the reductive half site reactions. Interestingly, Lux G, a flavin reductase from *Photobacterium leiognathi*, the reductase component of the class C two-component LuxAB monooxygenase system in bacterial luciferase, displayed similar reduction kinetics as the C_1-HPA system. [53]. Crystal structural studies may offer some insight into the deviation of reduction kinetics by FRED, from its related partner.

To monitor the re-oxidation activity of FRED, in the absence of monooxygenase, we investigated using sequential double mixing mode on the stopped flow to determine the effect of oxygen upon flavin reduction. Our results show a very rapid re-oxidation activity by the reductive component, which may not be due to any biological activity of the protein. The traces of re-oxidation is monophasic and is not accompanied by the detection of a C4a-(hydro)peroxyflavin intermediate although the oxygenating species for IBAH has been proposed to be through the formation of a C4a-(hydro)peroxyflavin [24]. Studies involving re-oxidation of reduced C_1-HPA showed biphasic traces in the presence and absence of HPA [39]. The monophasic behavior observed in both reduction and reoxidation experiments may support the earlier observation, about the absence of possible different isoforms of FRED, which therefore abolish a biphasic kinetic pattern. Further characterization of flavin reoxidation in HPAH system in the presence of both reductase and monooxygenase components observed the formation and stabilization of a C4a-hydroperxyflavin intermediate by His396 and Ser171 respectively [54]. Studies involving

flavin re-oxidation in the presence of both reductase and monooxygenase components will be necessary to establish the formation and stabilization of a possible intermediate.

Based on the kinetic data obtained, we propose a catalytic mechanism for the IBAH monooxygenase system (Scheme 1). The flavin reduction activity proceeds rapidly in 10 ± 0.2 s^{-1}. This rate is comparable to NADPH oxidation activity of FRED as measured in steady state kinetics that proceeded at 10.4 ± 0.5 s^{-1}. The reduction rate is reduced about 1.5-fold in the presence of IBA. The fate of $NADP^+$ whether bound or unbound is unknown, hence it is indicated as a product of the reduction reaction. Generally in class B monooxygenases, the $NADP^+$ has been shown to remain bound throughout the catalytic cycle for the purpose of stabilization of the C4a-(hydro)peroxyflavin oxygenating species [55-58]. The oxidation rate in comparison with the reduction rate is slow, ~ 5-fold decreased when IBAH binds in the presence of oxygen as measured from oxygen consumption assays. Reduced flavin reacts with oxygen, in the absence of monooxygenase without hydroxylation of substrate, at a rate of 4.79×10^{-9} $M^{-1}s^{-1}$. This re-oxidation activity is accompanied by the release of hydrogen peroxide. The rate measured by oxygen consumption is markedly reduced in the product formation assay due to the high degree of uncoupling ~ 99%. IBAH may be forming a complex with FAD and FRED, thereby, altering the kinetics of the overall reaction. The rate-limiting step, appears to be the oxidative half reaction. The transfer of flavin in the oxidative half may also dictate the reduced rate of reaction in the oxidative half. Detailed kinetic studies on the mechanism of flavin transfer may help deconvolute this assertion. The kinetic mechanism of the ActVA-ActVB system, a class D monooxygenase system from *Streptomyces coelicolor* has been determined. The reductive half reaction is slow followed

by a fast oxidative half reaction. The overall reaction is controlled by the reductive half reaction [59]. The proposed kinetic mechanism of the ActVA-VB monooxygenase system is consistent with the HPAH system [39, 60]. The overall mechanism in the IBAH monooxygenase system deviates from those proposed in both the ActVA-VB and HPAH systems. Kinetic data on fluorescence measurements and reductive half reactions were inconsistent with the HPAH system, it is therefore not surprising that, the overall reaction mechanism is inconsistent with those in related proteins.

The proposed reductive and oxidative mechanism of the IBAH monooxygenase system appears to differ from those in related ActVA-ActVB and HPAH systems. Sequence alignment data from previous work did not identify any proteins with significant similarities to IBAH and FRED [25, 31]. The very low sequence identity between these organisms (21 % for HPAH and 31% for ActVA-ActVB) suggests an evolutionary divergence of the IBAH monooxygenase system from related proteins. This offers some explanation into the different observations made especially in the proposed catalytic mechanism. In future work, data obtained can be used in further understanding of the reaction mechanism, allowing deeper insight into this emerging class of flavin-dependent monooxygenases.

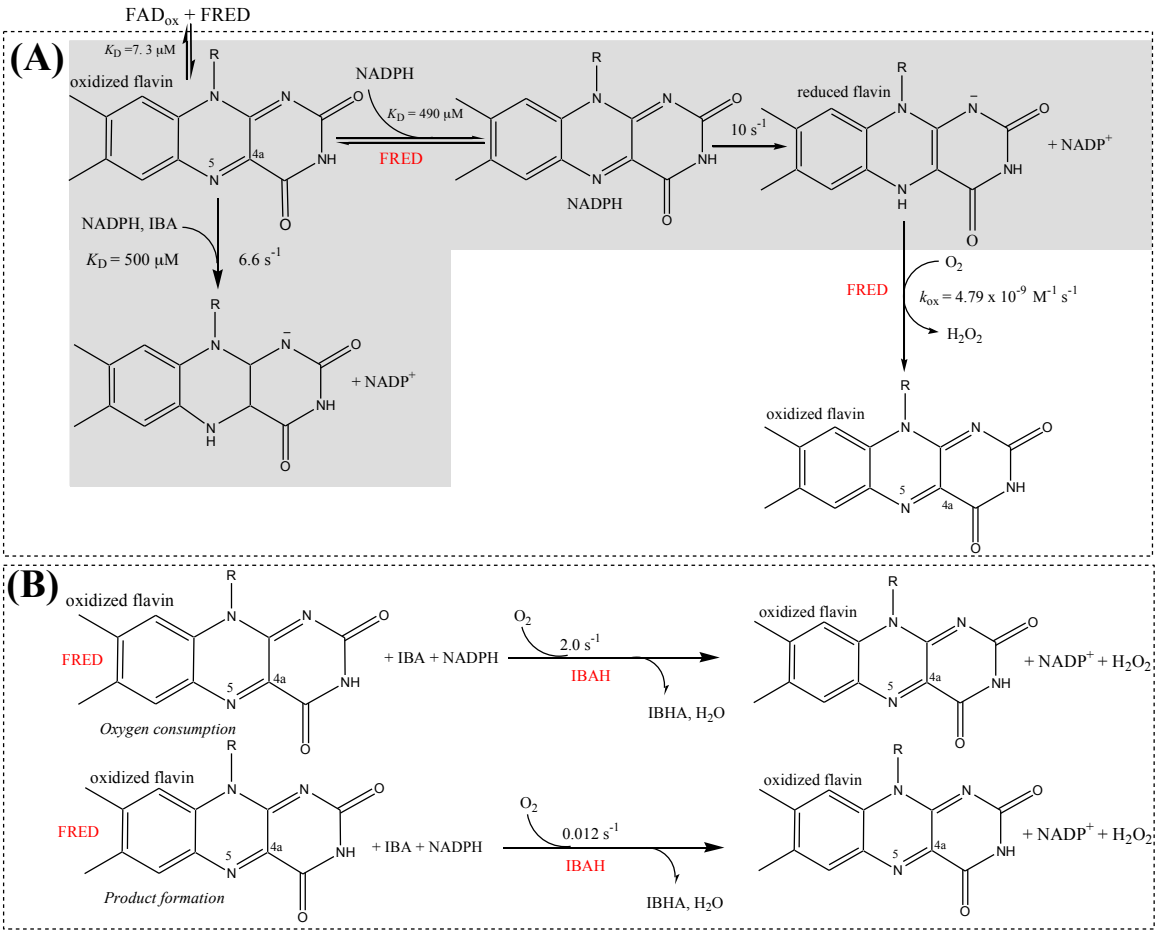

Scheme 1. Proposed catalytic mechanism for the IBAH two-component monooxygenase system. (A) FRED activity and (B) IBAH activity. The shaded region represents the reductive half reaction and the unshaded region represents the oxidative half reaction. Reduction proceeds rapidly and is decreased in the presence of substrate. The oxidative half reaction is ~5-fold slower than the reductive half and is highly uncoupled from substrate hydroxylation.

CHAPTER 5: Conclusion and future studies

5.1 Conclusion

The kinetic data presented in this thesis has offered important kinetic and chemical characterization on the IBAH monooxygenase system. IBAH and FRED were purified to homogeneity with no bound flavin. The IBAH monooxygenase system exhibited a high degree of uncoupling. In flavin reduction studies involving FRED, NADPH was the preferred substrate in comparison to NADH. IBA also does not serve as a substrate effector of FRED activity. The overall catalytic mechanism of the IBAH monooxygenase system is controlled by the oxidative half reaction and the mechanism proposed may suggest complex formation between the erductase and monooxygenase components which thereby alters the reaction kinetics.

5.2 Future studies

Future studies into the IBAH two-component systems would allow detailed explanations into some the observations made in this study. Monitoring of flavin re-oxidation in the presence of monooxygenase component would allow studies into the possible formation of an intermediate species, as well as the fate of $NADP^+$ in the catalytic cycle. Reduced flavin transfer mechanism studies would also offer explanations into the catalytic mechanism proposed. Crystal structure determinations of IBAH and FRED would provide helpful information on this enzyme system, and would be important for the class D monooxygenase and two-component systems in general, since structures of any member of this class is yet to be elucidated.

References

1. Huijbers, M.M., et al., *Flavin dependent monooxygenases*. Arch Biochem Biophys, 2014. **544**: p. 2-17.
2. Romero, E., et al., *Dual role of NADP(H) in the reaction of a flavin dependent N-hydroxylating monooxygenase*. Biochim Biophys Acta, 2012. **1824**(6): p. 850-7.
3. Cochrane, R.V. and J.C. Vederas, *Highly selective but multifunctional oxygenases in secondary metabolism*. Acc Chem Res, 2014. **47**(10): p. 3148-61.
4. Entsch, B. and W.J. van Berkel, *Structure and mechanism of para-hydroxybenzoate hydroxylase*. Faseb j, 1995. **9**(7): p. 476-83.
5. Massey, V., *Activation of molecular oxygen by flavins and flavoproteins*. J Biol Chem, 1994. **269**(36): p. 22459-62.
6. Sutton, W.B., *Mechanism of action and crystallization of lactic oxidative decarboxylase from Mycobacterium phlei*. J Biol Chem, 1957. **226**(1): p. 395-405.
7. Alfieri, A., et al., *Structure of the monooxygenase component of a two-component flavoprotein monooxygenase*. Proc Natl Acad Sci U S A, 2007. **104**(4): p. 1177-82.
8. Massey, V., *The chemical and biological versatility of riboflavin*. Biochem Soc Trans, 2000. **28**(4): p. 283-96.
9. van Berkel, W.J., N.M. Kamerbeek, and M.W. Fraaije, *Flavoprotein monooxygenases, a diverse class of oxidative biocatalysts*. J Biotechnol, 2006. **124**(4): p. 670-89.
10. Fraaije, M.W., et al., *Identification of a Baeyer-Villiger monooxygenase sequence motif*. FEBS Lett, 2002. **518**(1-3): p. 43-7.
11. Franceschini, S., et al., *Structural insight into the mechanism of oxygen activation and substrate selectivity of flavin-dependent N-hydroxylating monooxygenases*. Biochemistry, 2012. **51**(36): p. 7043-5.
12. Fitzpatrick, P.F., *Oxidation of amines by flavoproteins*. Arch Biochem Biophys, 2010. **493**(1): p. 13-25.
13. Chocklett, S.W. and P. Sobrado, *Aspergillus fumigatus SidA is a highly specific ornithine hydroxylase with bound flavin cofactor*. Biochemistry, 2010. **49**(31): p. 6777-83.
14. Mayfield, J.A., et al., *Comprehensive spectroscopic, steady state, and transient kinetic studies of a representative siderophore-associated flavin monooxygenase*. J Biol Chem, 2010. **285**(40): p. 30375-88.
15. Meneely, K.M. and A.L. Lamb, *Biochemical characterization of a flavin adenine dinucleotide-dependent monooxygenase, ornithine hydroxylase from Pseudomonas aeruginosa, suggests a novel reaction mechanism*. Biochemistry, 2007. **46**(42): p. 11930-7.
16. Tinikul, R., et al., *The transfer of reduced flavin mononucleotide from LuxG oxidoreductase to luciferase occurs via free diffusion*. Biochemistry, 2013. **52**(39): p. 6834-43.
17. Yeh, E., et al., *Chlorination by a long-lived intermediate in the mechanism of flavin-dependent halogenases*. Biochemistry, 2007. **46**(5): p. 1284-92.
18. Dong, C., et al., *Tryptophan 7-halogenase (PrnA) structure suggests a mechanism for regioselective chlorination*. Science, 2005. **309**(5744): p. 2216-9.

19. Ellis, H.R., *The FMN-dependent two-component monooxygenase systems*. Arch Biochem Biophys, 2010. **497**(1-2): p. 1-12.
20. Sucharitakul, J., R. Tinikul, and P. Chaiyen, *Mechanisms of reduced flavin transfer in the two-component flavin-dependent monooxygenases*. Arch Biochem Biophys, 2014. **555-556**: p. 33-46.
21. Arunachalam, U., V. Massey, and C.S. Vaidyanathan, *p-Hydroxyphenylacetate-3-hydroxylase. A two-protein component enzyme*. J Biol Chem, 1992. **267**(36): p. 25848-55.
22. Prieto, M.A. and J.L. Garcia, *Molecular characterization of 4-hydroxyphenylacetate 3-hydroxylase of Escherichia coli. A two-protein component enzyme*. J Biol Chem, 1994. **269**(36): p. 22823-9.
23. Chaiyen, P., C. Suadee, and P. Wilairat, *A novel two-protein component flavoprotein hydroxylase*. Eur J Biochem, 2001. **268**(21): p. 5550-61.
24. Parry, R.J. and W. Li, *Purification and characterization of isobutylamine N-hydroxylase from the valanimycin producer Streptomyces viridifaciens MG456-hF10*. Arch Biochem Biophys, 1997. **339**(1): p. 47-54.
25. Parry, R.J., W. Li, and H.N. Cooper, *Cloning, analysis, and overexpression of the gene encoding isobutylamine N-hydroxylase from the valanimycin producer, Streptomyces viridifaciens*. J Bacteriol, 1997. **179**(2): p. 409-16.
26. Hollmann, F., et al., *Stereospecific biocatalytic epoxidation: the first example of direct regeneration of a FAD-dependent monooxygenase for catalysis*. J Am Chem Soc, 2003. **125**(27): p. 8209-17.
27. Otto, K., et al., *Biochemical characterization of StyAB from Pseudomonas sp. strain VLB120 as a two-component flavin-diffusible monooxygenase*. J Bacteriol, 2004. **186**(16): p. 5292-302.
28. Valton, J., et al., *A two-component flavin-dependent monooxygenase involved in actinorhodin biosynthesis in Streptomyces coelicolor*. J Biol Chem, 2004. **279**(43): p. 44362-9.
29. Sucharitakul, J., et al., *Kinetic mechanisms of the oxygenase from a two-component enzyme, p-hydroxyphenylacetate 3-hydroxylase from Acinetobacter baumannii*. J Biol Chem, 2006. **281**(25): p. 17044-53.
30. Chakraborty, S., et al., *Studies on the mechanism of p-hydroxyphenylacetate 3-hydroxylase from Pseudomonas aeruginosa: a system composed of a small flavin reductase and a large flavin-dependent oxygenase*. Biochemistry, 2010. **49**(2): p. 372-85.
31. Parry, R.J. and W. Li, *An NADPH:FAD oxidoreductase from the valanimycin producer, Streptomyces viridifaciens. Cloning, analysis, and overexpression*. J Biol Chem, 1997. **272**(37): p. 23303-11.
32. Parry, R.J. and W. Li, *The biosynthesis of valanimycin. Further evidence for the intermediacy of a hydroxylamine in N-N bond formation*. Journal of the Chemical Society, Chemical Communications, 1994(8): p. 995-996.
33. Garg, R.P., et al., *Investigations of valanimycin biosynthesis: elucidation of the role of seryl-tRNA*. Proc Natl Acad Sci U S A, 2008. **105**(18): p. 6543-7.
34. Yamato, M., Iinuma, H, Naganawa, Y. Yamagishi, M. Hamada, T. Masuda and H. Umezawa, *Isolation and properties of valanimycin, a new azoxy antibiotic*. J . Antibiot., 1986. **39**: p. 184-191.

35. Robinson, R. and P. Sobrado, *Substrate binding modulates the activity of Mycobacterium smegmatis G, a flavin-dependent monooxygenase involved in the biosynthesis of hydroxamate-containing siderophores*. Biochemistry, 2011. **50**(39): p. 8489-96.
36. Fabiani, A., et al., *High-performance liquid chromatographic analysis of free amino acids in fruit juices using derivatization with 9-fluorenylmethyl-chloroformate*. J Chromatogr Sci, 2002. **40**(1): p. 14-8.
37. Heinrikson, R.L. and S.C. Meredith, *Amino acid analysis by reverse-phase high-performance liquid chromatography: precolumn derivatization with phenylisothiocyanate*. Anal Biochem, 1984. **136**(1): p. 65-74.
38. Binda, C., et al., *An unprecedented NADPH domain conformation in lysine monooxygenase NbtG provides insights into uncoupling of oxygen consumption from substrate hydroxylation*. J Biol Chem, 2015. **290**(20): p. 12676-88.
39. Sucharitakul, J., et al., *The reductase of p-hydroxyphenylacetate 3-hydroxylase from Acinetobacter baumannii requires p-hydroxyphenylacetate for effective catalysis*. Biochemistry, 2005. **44**(30): p. 10434-42.
40. Procopio, R.E., et al., *Antibiotics produced by Streptomyces*. Braz J Infect Dis, 2012. **16**(5): p. 466-71.
41. Brown, E.D. and G.D. Wright, *Antibacterial drug discovery in the resistance era*. Nature, 2016. **529**(7586): p. 336-43.
42. Li, J.W. and J.C. Vederas, *Drug discovery and natural products: end of an era or an endless frontier?* Science, 2009. **325**(5937): p. 161-5.
43. Dunne, E.F., W.J. Burman, and M.L. Wilson, *Streptomyces pneumonia in a patient with human immunodeficiency virus infection: case report and review of the literature on invasive streptomyces infections*. Clin Infect Dis, 1998. **27**(1): p. 93-6.
44. Moss, W.J., et al., *Streptomyces bikiniensis bacteremia*. Emerg Infect Dis, 2003. **9**(2): p. 273-4.
45. Kapadia, M., K.V. Rolston, and X.Y. Han, *Invasive Streptomyces infections: six cases and literature review*. Am J Clin Pathol, 2007. **127**(4): p. 619-24.
46. Kofteridis, D.P., et al., *Streptomyces pneumonia in an immunocompetent patient: a case report and literature review*. Diagn Microbiol Infect Dis, 2007. **59**(4): p. 459-62.
47. Jacob, F. and J. Monod, *Genetic regulatory mechanisms in the synthesis of proteins*. J Mol Biol, 1961. **3**: p. 318-56.
48. Studier, F.W., *Protein production by auto-induction in high density shaking cultures*. Protein Expr Purif, 2005. **41**(1): p. 207-34.
49. Vagenende, V., M.G. Yap, and B.L. Trout, *Mechanisms of protein stabilization and prevention of protein aggregation by glycerol*. Biochemistry, 2009. **48**(46): p. 11084-96.
50. Lee, J.K. and H. Zhao, *Identification and characterization of the flavin:NADH reductase (PrnF) involved in a novel two-component arylamine oxygenase*. J Bacteriol, 2007. **189**(23): p. 8556-63.
51. Barrio, J.R., et al., *Flavin 1, N 6 -ethenoadenine dinucleotide: dynamic and static quenching of fluorescence*. Proc Natl Acad Sci U S A, 1973. **70**(3): p. 941-3.

52. Becker, D., T. Schrader, and J.R. Andreesen, *Two-component flavin-dependent pyrrole-2-carboxylate monooxygenase from Rhodococcus sp*. Eur J Biochem, 1997. **249**(3): p. 739-47.
53. Nijvipakul, S., D.P. Ballou, and P. Chaiyen, *Reduction kinetics of a flavin oxidoreductase LuxG from Photobacterium leiognathi (TH1): half-sites reactivity*. Biochemistry, 2010. **49**(43): p. 9241-8.
54. Thotsaporn, K., et al., *Stabilization of C4a-hydroperoxyflavin in a two-component flavin-dependent monooxygenase is achieved through interactions at flavin N5 and C4a atoms*. J Biol Chem, 2011. **286**(32): p. 28170-80.
55. Beaty, N.B. and D.P. Ballou, *The oxidative half-reaction of liver microsomal FAD-containing monooxygenase*. J Biol Chem, 1981. **256**(9): p. 4619-25.
56. Sheng, D., D.P. Ballou, and V. Massey, *Mechanistic studies of cyclohexanone monooxygenase: chemical properties of intermediates involved in catalysis*. Biochemistry, 2001. **40**(37): p. 11156-67.
57. Torres Pazmino, D.E., et al., *Kinetic mechanism of phenylacetone monooxygenase from Thermobifida fusca*. Biochemistry, 2008. **47**(13): p. 4082-93.
58. Shirey, C., S. Badieyan, and P. Sobrado, *Role of Ser-257 in the sliding mechanism of NADP(H) in the reaction catalyzed by the Aspergillus fumigatus flavin-dependent ornithine N5-monooxygenase SidA*. J Biol Chem, 2013. **288**(45): p. 32440-8.
59. Valton, J., et al., *Mechanism and regulation of the Two-component FMN-dependent monooxygenase ActVA-ActVB from Streptomyces coelicolor*. J Biol Chem, 2008. **283**(16): p. 10287-96.
60. Sucharitakul, J., et al., *Kinetics of a two-component p-hydroxyphenylacetate hydroxylase explain how reduced flavin is transferred from the reductase to the oxygenase*. Biochemistry, 2007. **46**(29): p. 8611-23.